	Model Error Resolution Document *Complete only applicable items.*	QA: QA Page 1 of 50

1. Document Number:	MDL-NBS-HS-000010	2. Revision/Addendum:	03/01	3. ERD:	01
4. Title:	Site-Scale Saturated Zone Transport				
5. No. of Pages Attached:	49				

6. Description of and Justification for Change (Identify affected pages, applicable CRs and TBVs):

I Background Information Summary

This ERD is prepared to resolve CR 11825, CR 11020, CR12300, CR 12360, CR 12647, and TBV-8234 associated with *Site-Scale Saturated Zone Transport*, MDL-NBS-HS-000010 REV 03 AD 01. The errors identified in each of these condition reports and the TBV item are analyzed herein for potential impacts on the parent report, MDL-NBS-HS-000010 REV 03 AD 01, and downstream users.

I.1 CR 11825

CR 11825 identified the following errors in MDL-NBS-HS-000010 REV 03 AD 01, Table 4-1, both in the last row of the table on p. 4-2 of the parent report, corresponding to DTN: LA0305AM831341.001:

- Left column: Americium, protactinium, and thorium were omitted from the list of elements.
- Right column: For the eight files identified, the word "Rations" should be "Ratios."

(continued on next page)

7. CONCURRENCE			
	Printed Name	Signature	Date
Checker	Charles Haukwa		01/13/2009
QCS/QA Reviewer	Peter Persoff		01/13/2009
8. APPROVAL			
Originator	Sharad Kelkar		01/13/2009
Responsible Manager	Robert MacKinnon		01/13/2009

(Continued from Block 6)

During the extent of condition investigation of CR 11825, the following additional errors were noted in Table 4-1 of MDL-NBS-HS-000010 REV 03 AD 01:

- Row for Cesium, entry for LA0407AM831341.002: file name missing in the right column
- Row listing DTN: MO0007MAJIONPH.011: description incorrect in the left column
- Row listing DTN: LAJC831321AQ98.005: table name incorrect in the right column
- Row for MO0101XRDMINAB.001: table names missing in the right column
- Row for MO0106XRDDRIL.003: table names missing in the right column
- Row for MO0101XRDDRILC.002: table names missing in the right column
- DTN: LA0302MD831341.003 [DIRS 163784], *Np-237.txt* and DTN: LA0302MD831341.004 [DIRS 163785], *U-233.doc* are listed in the same cell as LA0305AM831341.001 [DIRS 163789]. However, those two DTNs contain data for K_d values measured on alluvium, not tuff. They should have a separate description.
- File name corresponding to DTN: MO0408K8313211.000 [DIRS 171437] is incorrect.

The following additional errors were noted in Section 9.3 of MDL-NBS-HS-000010 REV 03 AD 01:

- Entry corresponding to the DTN: MO0007MAJIONPH.011 [DIRS 151524]: the reference description is inconsistent with that in the DIRS.

I.2 CR 11020

CR 11020 identified the following errors in DTN: LA0305AM831341.001, *1977 to 1987 Sorption Measurements of Am, Ba, Cs, Np, Pu, Pa, Sr, Th, and U with Yucca Mountain Rock Samples*: rock-type classifications for some tuff samples contained in this DTN are internally inconsistent or inconsistent with other data.

- One tuff sample (G1-2698) is classified as devitrified in the DTN. However, report LA-11669-MS [DIRS 101374], Appendix I, p. 15, reports an XRD analysis that would make it zeolitic.
- Three other samples are given different classifications in different places within the DTN:
  - Sample G1-2689 is described as both devitrified and zeolitic in the spreadsheet for U, and as zeolitic on spreadsheets for other elements.

- Sample JA-18 is described as zeolitic on the spreadsheet for Am, but vitric on the spreadsheets for U and Pu.

- Sample G1-3116 is described as devitrified on the spreadsheet for Th, but zeolitic on the spreadsheets for other elements.

During the extent of condition investigation of CR 11020, the following additional errors were noted in DTN: LA0305AM831341.001:

- Errors in sorption and pH data listed for strontium in experiments using p#1 water
- Errors in rock sample identifiers
- Errors in lithostratigraphic unit designations
- Errors in particle size ranges
- Errors in reported pH values
- Duplicate data rows
- Errors and missing entries for tracer concentrations
- Incorrect and inadequate traceability for data sources.

Errors were also noted in DTN: LA0310AM831341.001, *Sorption/Desorption Measurements of Cesium on Yucca Mountain Tuff*:

- Errors in rock sample identifiers
- Errors in lithostratigraphic unit designations
- Error in formulas used to calculate final element concentration
- Incorrect and inadequate traceability for data sources

Additionally, an error in rock-type classification was noted in DTN: LA0407AM831341.005, *Batch Sorption Coefficient Data for Plutonium on Yucca Mountain Tuffs in Representative Water Compositions*:

- Sample G4-272 is described as zeolitic but should be devitrified.

Other errors noted in DTN: LA0407AM831341.005 include:

- Incorrect and inadequate traceability for data sources
- Errors in lithostratigraphic unit designations
- Errors in experiment sample identifiers
- Errors in reported pH values
- Duplicate data rows
- No readme file
- Error in material mass listed for one sample, leading to an error in calculated K_d value.

The following additional error was noted in Figures A-35 and H-1: the point with the highest value for "Sorption J-13 New" data, denoted by open squares in the figures, is not listed in the source DTNs.

I.3 CR 12300

CR 11731 identified that ANL-NBS-HS-000039 REV 02 [DIRS 177394] had two sections numbered 6.5.5. In corrective action 11731-001, the second Section 6.5.5 was renumbered as 6.5.6, and all following subsections within 6.5 were also incremented. As a result, other documents that cite these subsections of ANL-NBS-HS-000039 REV 02 [DIRS 177394] are now in error, and the citations must be corrected.

This affected MDL-NBS-HS-000010 REV 03 AD 01 and the necessary changes were identified in ANL-NBS-HS-000039 ERD 01, Section IV.1:

- p. 6-2, halfway down page, citation to DIRS 177394, Section 6.5.6 should be changed to Section 6.5.7.
- p. 7-20, 4th line from bottom, citation to DIRS 177394, Section G5.4.3 should be changed to Section G5.4.4.

I.4 CR 12360

CR 12360 identified an incorrect statement presented in Section 6.4.2 of MDL-NBS-HS-000010 REV 03 AD 01. Equation 2 in that section presents the Burnett and Frind form of dispersion tensor, and the discussion following Equation 2 states that this is the form used in the SZ transport model. Instead, Equation A1 of Tompson et al. (1987 [DIRS 145195]) is used as the starting point of the development presented in Section 6.4.2 of MDL-NBS-HS-000010 REV 03 AD 01.

Correction of this error is accomplished in Attachment A of this ERD, which reproduces the relevant subsections of Section 6.4.2 and incorporates the necessary changes.

I.5 CR 12647

CR 12647 addressed a subset of the errors during resolution of CR 11020: This CR noted that four rock type misclassifications in DTN: LA0803AM831341.002 were not corrected as intended in response to closed CR action item 11020-001. These errors were corrected via supersession of this source DTN. ERD corrections related to CR 12647 and CR 11020 are addressed together in Section III.2.

I.6 TBV-8234

TDR-CRW-HS-000001 REV 00 [DIRS 184177] has been approved. It was noted that DTN: LA0702AM831341.001 [DIRS 179306] contained two data values with transcription errors, and the rock type classification of the samples G1-2233, G1-2289, G1-3116, G2-0547, GU3-1531, and GU3-433 was stated incorrectly.

I.7 Other Issues

During development of the ERD, one issue was identified concerning inadequate traceability for data sources for Table A-3. Table A-3 of the parent report MDL-NBS-HS-000010 REV 03 AD

01 has a source DTN: LA0702MD831232.001. However, the report does not provide the name of the specific data file. The documentation needs to provide clear traceability.

II Inputs and/or Software

Direct inputs to these corrections include the following DTNs in addition to those listed in MDL-NBS-HS-000010 REV 03 AD 01:

- LA0803AM831341.001 [DIRS 185573]
- LA0809AM831341.003 [DIRS 185783].

DTN: LA0803AM831341.001 [DIRS 185573] is qualified in Appendix H as amended in this ERD. DTN: LA0809AM831341.003 [DIRS 185783] is qualified as shown in the TDMS.

No software controlled under IM-PRO-003, *Software Management*, is used in these corrections.

No new software was used.

III Analysis and Changes

III.1 Analysis and Changes for CR 11825

III.1.1 Analysis

CR 11825 identifies two issues concerning Table 4-1 of MDL-NBS-HS-000010 REV 03 AD 01. Additional corrections associated with it and with CR 11020 and CR 12647, as described in the section above, are presented below.

III.1.2 Changes to MDL-NBS-HS-000010 REV 03 AD 01

Note that the corrections made to Table 4-1 and Section 9 to resolve CR 11825 were coordinated with corrections made to resolve CR 11020, and CR 12647, described in Section III.2. Entries for the following DTNs have been modified:

- LA0407AM831341.002 [DIRS 170621]
- LA0407AM831341.005 [DIRS 170625]
- LA0305AM831341.001[DIRS 163789]
- LAJC831321AQ98.005 [DIRS 109004]
- MO0408K8313211.000 [DIRS 171437]
- MO0007MAJIONPH.011 [DIRS 151524]
- MO0101XRDMINAB.001 [DIRS 163796]
- MO0106XRDDRILC.003 [DIRS 163797]
- MO0101XRDDRILC.002 [DIRS 163795]
- LA0302MD831341.003 [DIRS 163784]
- LA0302MD831341.004 [DIRS 163785].

III.1.2.1 Corrected Table 4-1

The following shows the corrected Table 4-1 of MDL-NBS-HS-000010 REV 03 AD 01:

Table 4-1. Input Data and Technical Information

Data Description	Source/ Data Tracking Number and *Filename*
Data and Technical Information for Uncertainty Distribution of Parameters	
Uncertainty distribution for parameters used in the saturated zone transport abstractions model	SN0310T0502103.009 [DIRS 168763], *DTN-SN0310T0502103.009.zip\Table 6-8_updated.doc,* SN0706INPUTSZF.000 [DIRS 182007], file *updated_SZ_inputs_table.doc*
Data and Technical Information for Base-Case Flow Model	
FEHM V2.24 files for base-case saturated zone site-scale flow model	SN0612T0510106.004 [DIRS 178956], *SZ Flow Model.zip*
Data and Technical Information for Sorption Coefficient Data	
Thermodynamic database for PHREEQC modeling calculation of radionuclide sorption coefficient	MO0604SPAPHR25.001[DIRS 176868], *phreeqcDATA025.dat*
Americium, protactinium, plutonium, and thorium sorption coefficients on silica and surface area for silica sample	Allard et al. 1983 [DIRS 162982], pp. 6, 9, 10, 12; Allard et al. 1980 [DIRS 104410], p. 478; Beall et al. 1986 [DIRS 162983], entire document. See Appendix L, Sections L1, L2, and L7 for qualification of the data
Density of sorption sites on the solid surface; uranium and neptunium surface complexation binding constants on silica	Pabalan et al. 1998 [DIRS 162987], p. 124 See Appendix L, Section L3 for qualification of the data
Batch sorption coefficient data for barium on Yucca Mountain tuffs in representative water compositions	LA0407AM831341.001 [DIRS 170623], *BARIUM(RIT).xls*
Batch sorption coefficient data for cesium on Yucca Mountain tuffs in representative water compositions	LA0407AM831341.002 [DIRS 170621], *CESIUM(RIT).xls*
Batch sorption coefficient data for strontium on Yucca Mountain tuffs in representative water compositions	LA0407AM831341.003 [DIRS 170626], *STRONTIUM(RIT).xls*
Batch sorption coefficient data for neptunium on Yucca Mountain tuffs in representative water compositions	LA0407AM831341.004 [DIRS 170622], *NEPTUNIUM(RIT).xls*
Batch sorption coefficient data for plutonium on Yucca Mountain tuffs in representative water compositions	LA0809AM831341.003 [DIRS 185797], LA0809AM831341_003 *Plutonium(RIT).xls*
Batch sorption coefficient data for uranium on Yucca Mountain tuffs in representative water compositions	LA0407AM831341.006 [DIRS 170628], *URANIUM(RIT).xls*
Batch sorption coefficients on Yucca Mountain tuffs for americium, barium and radium, cesium, neptunium, protactinium, plutonium, strontium, thorium, and uranium	LA0803AM831341.001[DIRS 185573], *LA0803AM831341-001 10-Jun-08.xls* (Data are qualified in Appendix H, as amended by this ERD)
Neptunium-237 sorption in alluvium	LA0302MD831341.003 [DIRS 163784], *Np-237.txt*
Uranium sorption in alluvium	LA0302MD831341.004 [DIRS 163785], *U-233.doc*
Water chemistry including pH for p#1 water	MO0007MAJIONPH.011 [DIRS 151524]

Table 4-1. Input Data and Technical Information

Data Description	Source/ Data Tracking Number
Data and Technical Information for Sorption Coefficient Data (Continued)	
Fluorine abundance data from ue-25 p#1 taken on February 09,1983	SN0705FLUORINE.001 [DIRS 182006] (data qualified in appendix M)
Deprotonation constants and binding constants for aluminum and silica	Dixit and Van Cappellen 2002 [DIRS 162985], p. 2,565 See Appendix L, Section L5 for qualification of the data
Binding constants for sodium on silica	Marmier et al. 1999 [DIRS 162986], p. 228 See Appendix L, Section L6 for qualification of the data
Binding constants for neptunium on silica	Turner et al. 1998 [DIRS 162989], p. 264 See Appendix L, Section L4 for qualification of the data
Water compositions for samples from wells J-13 and p#1	Ogard and Kerrisk 1984 [DIRS 100783] Data are qualified in Appendix I
Se (selenium) and Sn (tin) sorption on Yucca Mountain rock samples.	LA0802AM831341.002 [DIRS 185081], *Se Sn DTN.R1.xls*
Colloid retardation factors for the Saturated Zone Alluvium	LA0303HV831352.004 [DIRS 163559], *Alluvium_retardation.txt*
Boundary of the Accessible Environment at 18 km	
Boundary of the accessible environment	10 CFR 63.302 [DIRS 180319] See NOTES for the justification of the use of the data
Data and Information for Stochastic Modeling of K_d	
Mineralogic data for Yucca Mountain.	LASC831321AQ98.001 [DIRS 109047], Table S98084_002
XRD data describing mineralogic composition of core samples from wells	Chipera et al. 1995 [DIRS 111081], entire document LA000000000086.002 [DIRS 107144], Table S97218_001
XRD data describing mineralogic composition of core samples from wells	LAJC831321AQ98.005 [DIRS 109004], Tables S98436_001, S98436_002, S98436_003, and S98436_004. LASC831321AQ98.001 [DIRS 109047], Table S98084_002 LADV831321AQ99.001 [DIRS 109044], Tables S99203_001, and S99203_002 MO0408K8313211.000 [DIRS 171437], Table S04337_001
XRD data describing mineralogic composition of core samples from wells	MO0101XRDMINAB.001 [DIRS 163796], Tables S01023_002, S01023_003, S01023_004, and S01023_005 MO0106XRDDRILC.003 [DIRS 163797], Table S01074_001 MO0101XRDDRILC.002 [DIRS 163795], Tables S01026_001 and S010626_002

Table 4-1. Input Data and Technical Information

Data Description	Source/ Data Tracking Number
Data and Information for Stochastic Modeling of K_d (Continued)	
Values of diffusion coefficients used for stochastic analysis	LA0003JC831362.001 [DIRS 149557], Table S00230_001 (Data qualified in Appendix K)
Hydraulic gradient used in stochastic modeling on a 550-m block	LA0511SK831214.001 [DIRS 175769], *hydraulic.zip*

NOTES: The accessible environment is any point outside of the controlled area, which must not extend farther south than 36°40'13.6661" North latitude, in the predominant direction of ground-water flow" in 10 CFR 63.302 [DIRS 180319]. This latitude is approximately 18 km south of the southern boundary of the repository footprint. It is referred to as the 'boundary to the accessible environment at 18 km' in this report, and it is used as an input to the site-scale SZ transport model for calculating BTCs. Any radionuclides crossing the vertical east-west plane across the entire site-scale SZ flow model, 18 km downstream from the repository footprint, are counted as breakthrough particles. This boundary is established by 10 CFR 63.302 [DIRS 180319], which, as a code of federal regulations, is judged to be an established fact.

EWDP = Early Warning Drilling Program; XRD = X-ray diffraction.

III.1.2.2 Correction to Section 9.3

Entry corresponding to DTN: MO0007MAJIONPH.011 [DIRS 151524] is changed to read as follows:

151524 MO0007MAJIONPH.011. Major Ion Content of Groundwater from Selected Yucca Mountain Project Boreholes. Submittal date: 07/27/2000.

III.2 Analysis and Changes for CR 11020 and CR 12647

III.2.1 Analysis

CR 11020 and CR 12647 identify issues concerning rock type classification in DTNs which are direct inputs to Appendix A of MDL-NBS-HS-000010 REV 03 AD 01. The resolution of CR 11020 and CR 12647 resulted in the supersession of the three DTNs: LA0305AM831341.001, LA0310AM831341.001, and LA0407AM831341.005 by two superseding DTNs: LA0803AM831341.001 and LA0809AM831341.003, as well as the creation of new DTN: LA0803SL831341.001. These changes are described below:

- DTN: LA0305AM831341.001 (titled "1977 to 1987 Sorption Measurements of Am, Ba, Cs, Np, Pu, Pa, Sr, Th, and U with Yucca Mountain Tuff Samples) and DTN: LA0310AM831341.001 (titled "Sorption/Desorption Measurements of Cesium on Yucca Mountain Tuff") were superseded by new DTN: LA0803AM831341.001 (titled "1977 to 1987 Sorption Measurements of Am, Ba, Cs, Np, Pu, Pa, Sr, Th, and U with Yucca Mountain Tuff Samples"). The following are results of the analysis resulting from these changes:

  – Reassignment of the rock-type for sample JA-18 from zeolitic to vitric. This change required the removal of sorption and desorption K_d values associated with this sample in Figure A-5, and deletion of the sentences referencing sample JA-18

in the first paragraph of Section A7.1.2. The legend of the revised Figure A-5 was also edited to correct a typographical error in two sample identifiers. The K_d distributions remain unchanged.

- Correction to calculated final Cs concentration in solution, reported in Column O of the superseding DTN LA0803AM831341.001. This change required corrections to Sections A7.2.1, A7.2.2, Figure A-8 and Figure A-11. Additionally, editorial changes were made to the source descriptions for Figures A-8 and A-9 to reflect that the cited data were shifted by one column in the superseding DTN. The K_d distributions remain unchanged.

- Correction of calculated values K_d and the calculated final Sr concentration in solution for sample G1-2901. This resulted in revision of Section A7.8.1 and the figures A-42, A-43, and A-44, as discussed below. Figures A-43 and A-44 also include point (63, 290) which was mistakenly omitted in the previous version of the figure. This point falls within the range of the data already plotted in the figure. The K_d distributions remain unchanged.

- Correction of the rock type for sample G1-3116 from devitrified to zeolitic. Hence, Section A7.9.1 and Figures A-49 and A-50 were revised to reflect these changes, as discussed below. Silica samples are added to Figure A-49. The calculated Th concentrations for the silica are lower than those of vitric Tuff, Devitrified Tuff, and Zeolitic Tuff, but K_d range is the same. The K_d distributions remain unchanged.

- Correction of the rock type for sample G1-2698 from devitrified to zeolitic. Hence, Sections A7.11.1 and A7.11.2, as well as Figures A-53 through A-60, were revised. The K_d distributions remain unchanged.

- Figure A-60 was modified to include point (9.16, 6.01), which was mistakenly omitted in the previous version of the figure. Point (9.16, 6.01) falls within the range of the data already plotted in the figure. The text explaining Figure A-60 remains valid. The K_d distributions remain unchanged.

- The text of Appendix H 'Qualification of Sorption Data' as well as Figures H-1 and H-2 were corrected to represent the data in the superseding DTNs as discussed below. The conclusions of the appendix to qualify the data remain unchanged.

- DTN: LA0407AM831341.005 (titled "Batch Sorption Coefficient Data for Plutonium on Yucca Mountain Tuffs in Representative Water Compositions") was superseded by new DTN: LA0809AM831341.003 (titled "Batch Sorption Coefficient Data for Plutonium on Yucca Mountain Tuffs in Representative Water Compositions").

  - Correction of the rock type for sample G4-272 from zeolitic to devitrified for four K_d values obtained using J-13 water in sorption and desorption experiments

lasting about 14 days. Corrections were made to Sections A7.4.1 and A7.4.2, Figures A-21 through A-24, and Figures A-26 through A-28. Figure A-21 was also revised to include the plotting category, "New Sorption p#1 > 40 Days," which had been left out of the original figure. The K_d distributions are unchanged.

- New DTN: LA0803SL831341.001 (titled "X-Ray Diffraction Analyses of Samples Used for Sorption Studies") was created in order to provide clear traceability to the most reliable and complete data set used to assign rock-type classifications. This DTN is based on XRD analysis of Yucca Mountain core samples collected from boreholes UE25 J-13, UE25 a#1, USW G-1, USW G-2, USW G-3, USW GU-3, and USW G-4 as documented in Los Alamos National Laboratory Report LA-11669-MS (ACC# NNA.19890414.0062) as well as data from XRD analysis of additional samples from boreholes USW GU-3 and USW G-1 as documented in the records road map for the DTN. : LA0803SL831341.001.

- An error was noted in Figure A-35: the point with the highest value for "Sorption J-13 New" data, denoted by open squares in the figures, is not listed in the source DTNs. This point was removed from the Figure A-35. The data ranges remain the same. The K_d distribution remains unchanged.

III.2.2 Changes to MDL-NBS-HS-000010 REV 03 AD 01

Note that corrections made to resolve CR 11020 and CR 12647 were coordinated with corrections made to resolve CR 11825, described in Section III.1.2. Also, note that the data from the DTN LA0803AM831341.001 [DIRS 185573] are called 'old' in the figure, the rest of the data are called 'new'.

III.2.2.1 Corrections to Footnotes to Figures in Sections A7.1, A7.3 through A7.6, A7.8, A7.9, and A7.11

Figures A-1 through A-3, A-5 through A-7, A-14 through A-35, A-42 through A-50, and A-53 through A-60 contain a footnote that lists as a source DTN: LA0305AM831341.001 [DIRS 163789]. This DTN has been superseded by DTN: LA0803AM831341.001 [DIRS 185573]. Hence, the portion of the footnote for all these figures is modified as follows:

Sources: DTNs: LA0803AM831341.001 [DIRS 185573];

III.2.2.2 Corrections to Section A7.1.2, p. A-15

The first paragraph of Section A7.1.2 and Figure A-5 are replaced by the following:

The measured sorption coefficients for zeolitic tuff are plotted versus calculated final solution concentrations in Figure A-5[b]. Although sorption experiments with sample G4-1952 were close to saturation with $AmOHCO_3$, the sorption coefficients obtained for this sample are used in the derivation of the distribution because the plotted data fit well with the overall trend.

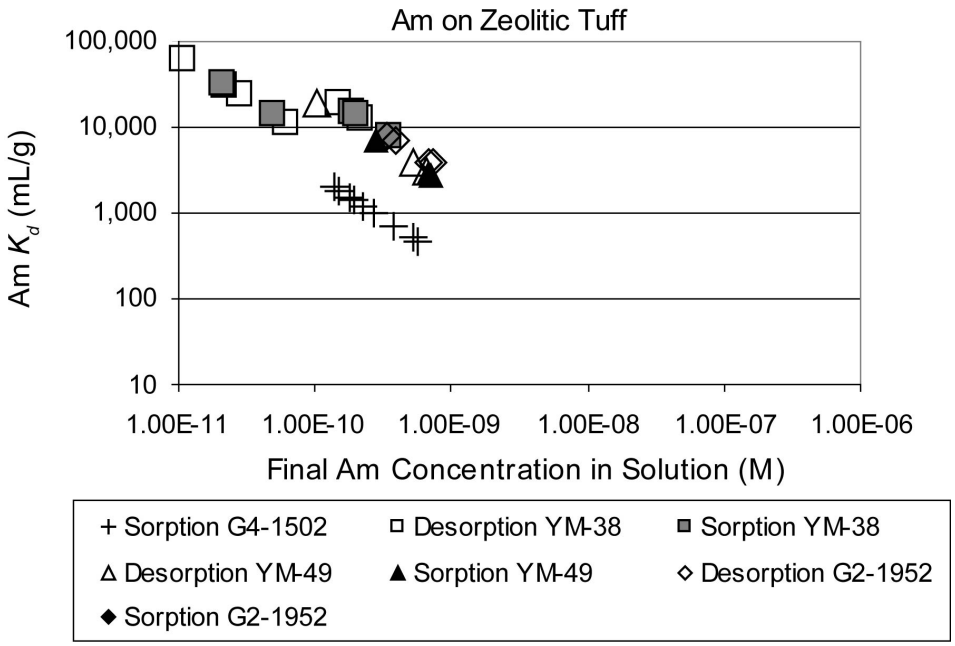

Source: DTN: LA0803AM831341.001 [DIRS 185573].

Figure A-5[b]. Americium Sorption Coefficients on Zeolitic Tuff versus Calculated Final Americium Concentration in Solution

III.2.2.3 Corrections to Section A7.2.1 and A7.2.2, pp. A-19 and A-22

Figures A-8 and A-11 are replaced by the following:

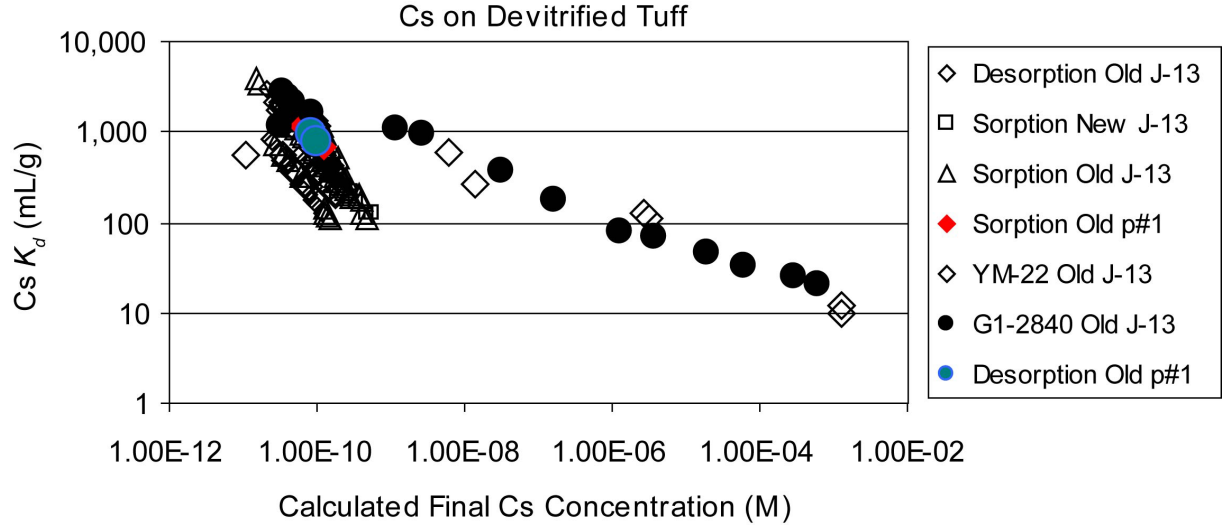

Sources: DTNs: LA0803AM831341.001 [DIRS 185573] (Column C and Column O); LA0407AM831341.002 [DIRS 170621] (Column N and Column P).

Figure A-8[b]. Cesium Sorption Coefficients on Devitrified Tuff versus Calculated Final Cesium Concentration in Solution

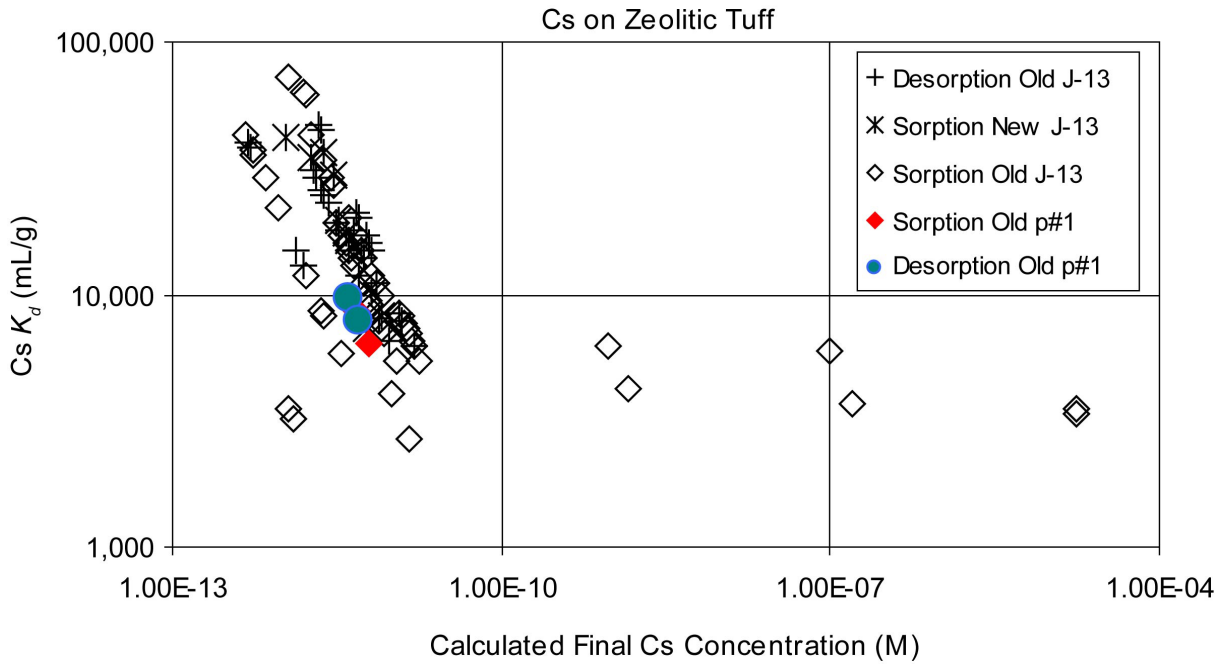

Sources: DTNs: LA0803AM831341.001 [DIRS 185573]; LA0407AM831341.002 [DIRS 170621].

NOTE: In the legend, 'old' stands for data collected before May 1989, 'new' stands for data collected after May 1989.

Figure A-11[b]. Cesium Sorption Coefficients on Zeolitic Tuff versus Calculated Final Cesium Concentration in Solution

III.2.2.4 Corrections to Section A7.4.1, pp. A-33 through 37

Figures A-21, A-22, A-23, and A-24 are replaced by the following:

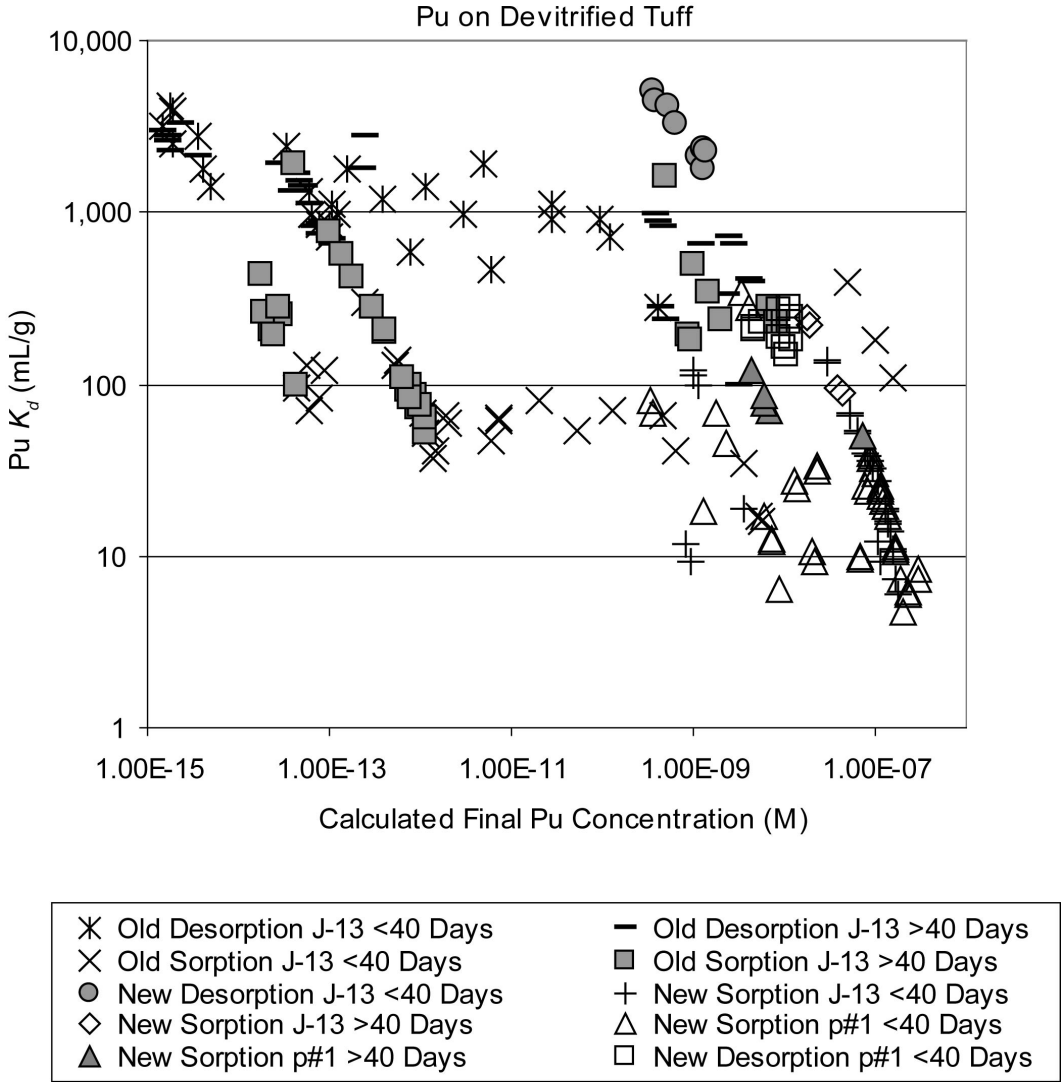

Sources: DTNs: LA0803AM831341.001 [DIRS 185573]; LA0809AM831341.003 [DIRS 185783].

NOTE: In the legend, 'old' stands for data collected before May 1989, 'new' stands for data collected after May 1989.

Figure A-21[b]. Plutonium Sorption Coefficients on Devitrified Tuff versus Calculated Final Plutonium Concentration in Solution

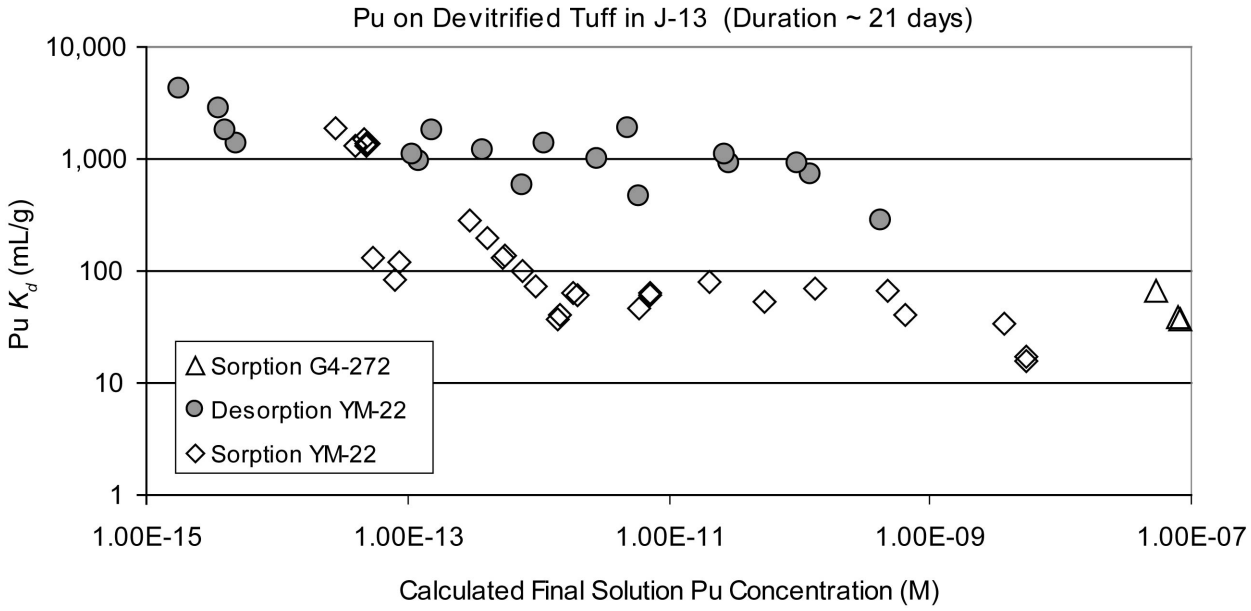

Sources: DTNs: LA0803AM831341.001 [DIRS 185573]; LA0809AM831341.003 [DIRS 185783].

Figure A-22[b]. Plutonium Sorption Coefficients versus Calculated Final Plutonium Solution Concentration (M) for Experiments with Samples YM-22 and G4-272

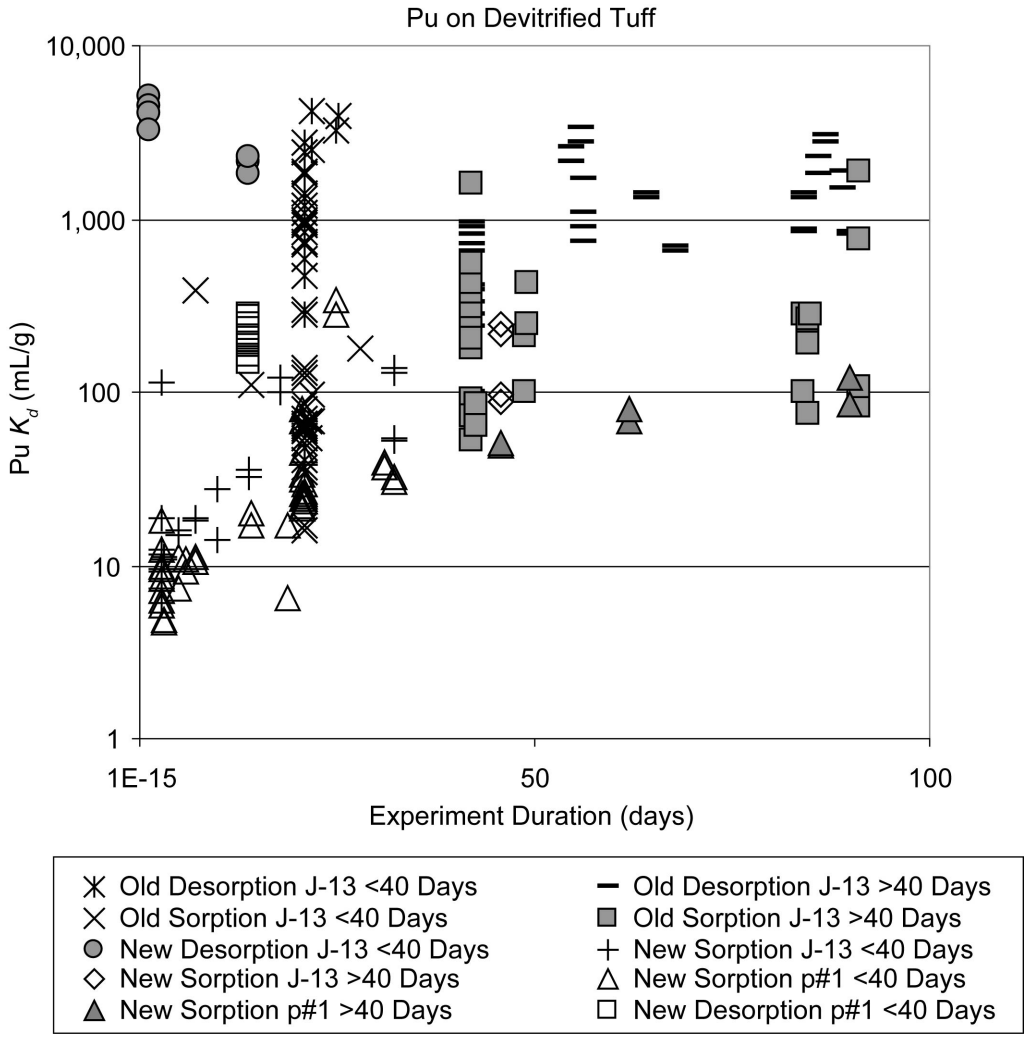

Sources: DTNs: LA0803AM831341.001 [DIRS 185573]; LA0809AM831341.003 [DIRS 185783].

Figure A-23[b]. Plutonium Sorption Coefficients on Devitrified Tuff versus Experiment Duration for Sorption (Forward) and Desorption (Backward) Experiments

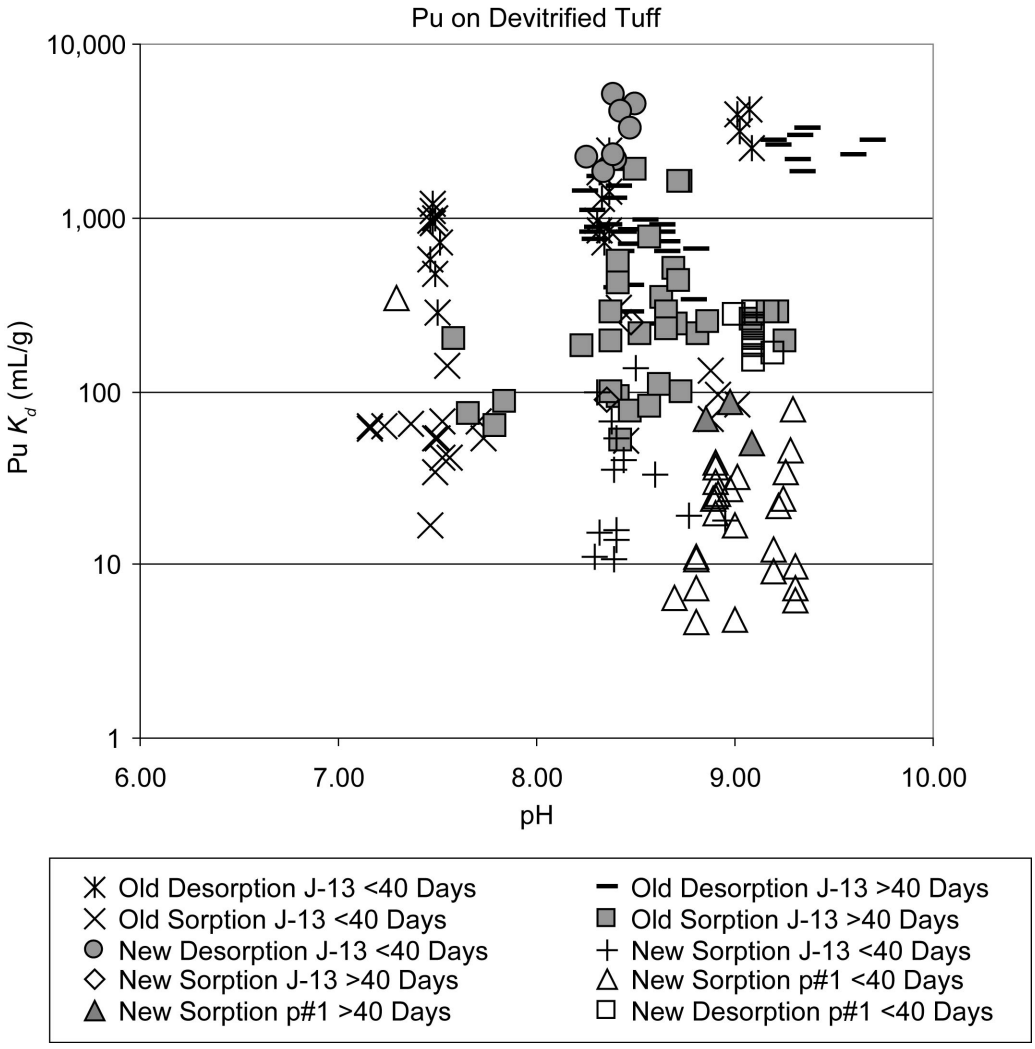

Sources: DTNs: LA0803AM831341.001 [DIRS 185573]; LA0809AM831341.003 [DIRS 185783].

NOTE: In the legend, 'old' stands for data collected before May 1989, 'new' stands for data collected after May 1989.

Figure A-24[b]. Plutonium Sorption Coefficients on Devitrified Tuff in J-13 Well Water and Synthetic p#1 Water versus Solution pH in Sorption (Forward) and Desorption (Backward) Experiments

III.2.2.9 Corrections to Section A7.4.2, pp. A-39 through A-42

Figures A-26, A-27, and A-28 are replaced by the following:

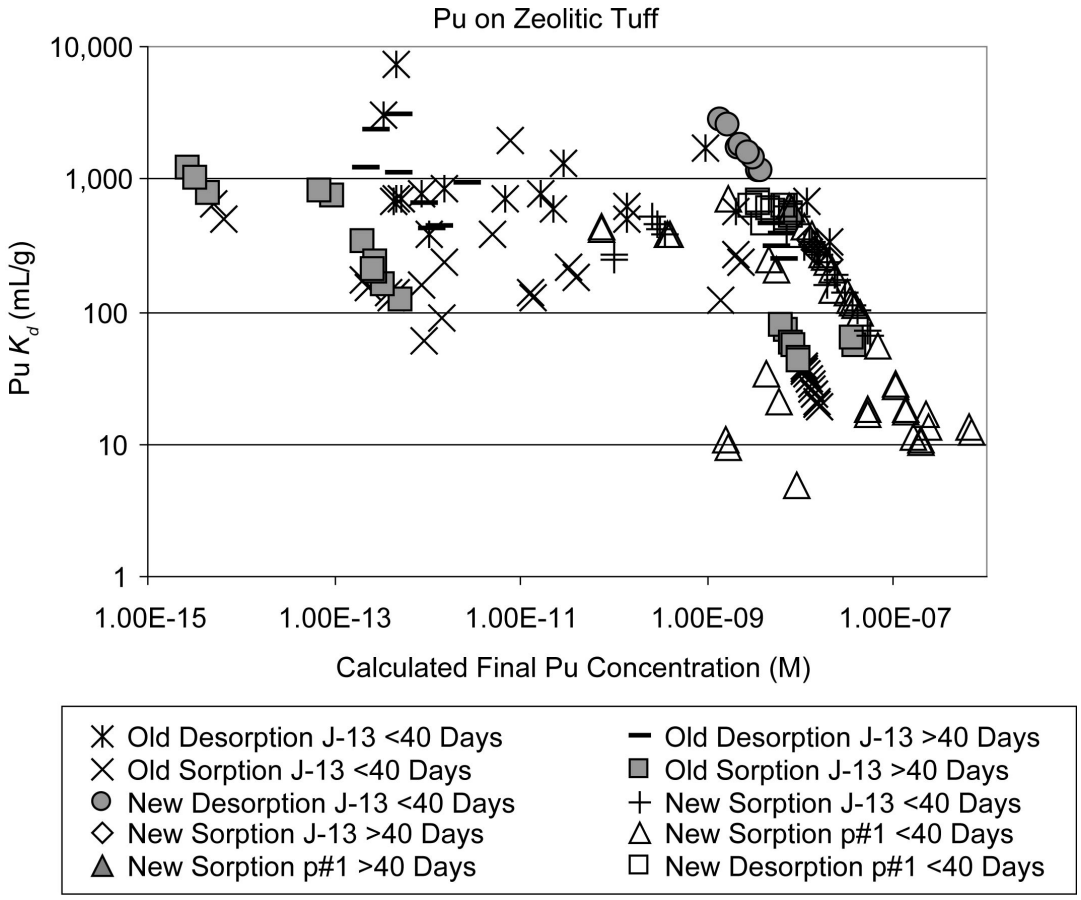

Sources: DTNs: LA0803AM831341.001 [DIRS 185573]; LA0809AM831341.003 [DIRS 185783].

NOTE: In the legend, 'old' stands for data collected before May 1989, 'new' stands for data collected after May 1989.

Figure A-26[b]. Plutonium Sorption Coefficients on Zeolitic Tuff versus Calculated Final Plutonium Concentration in Solution

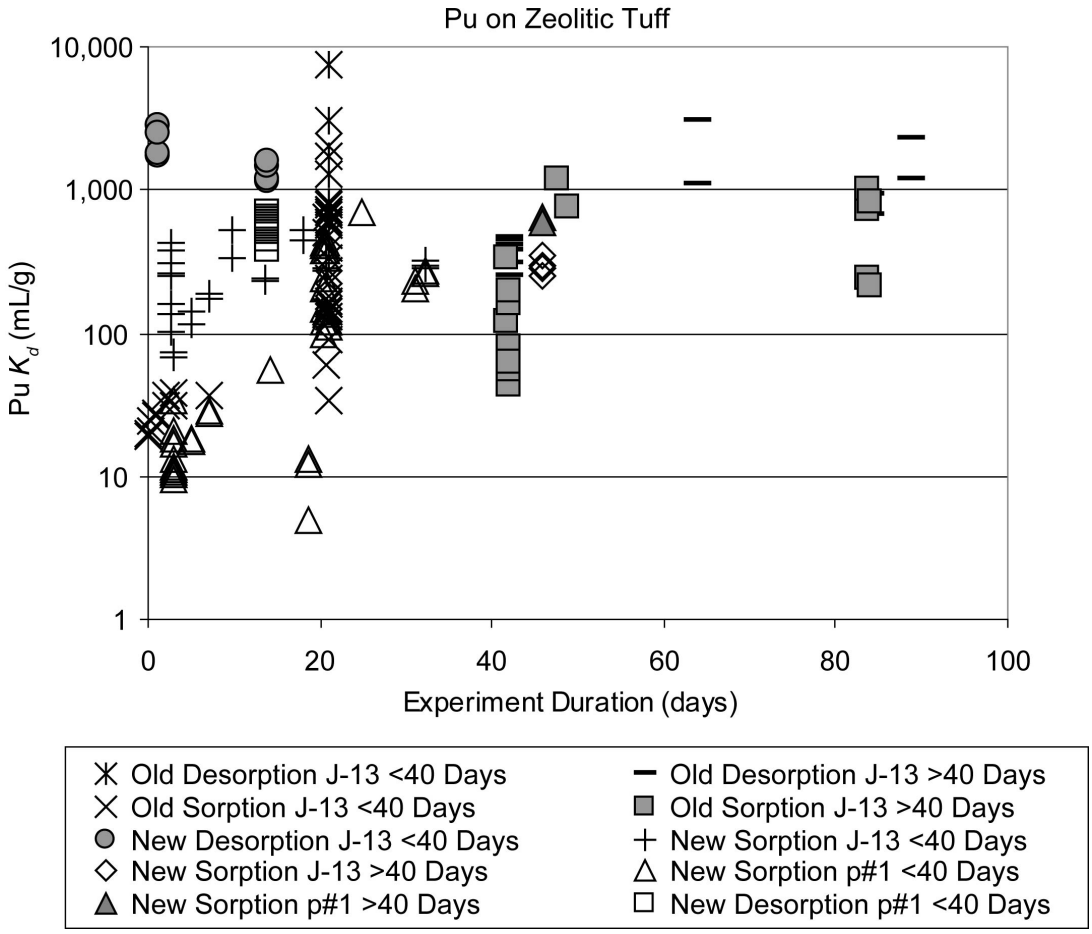

Sources: DTNs: LA0803AM831341.001 [DIRS 185573]; LA0809AM831341.003 [DIRS 185783].

NOTE: In the legend, 'old' stands for data collected before May 1989, 'new' stands for data collected after May 1989.

Figure A-27[b]. Plutonium Sorption Coefficients on Zeolitic Tuff versus Experiment Duration for Sorption (Forward) and Desorption (Backward) Experiments

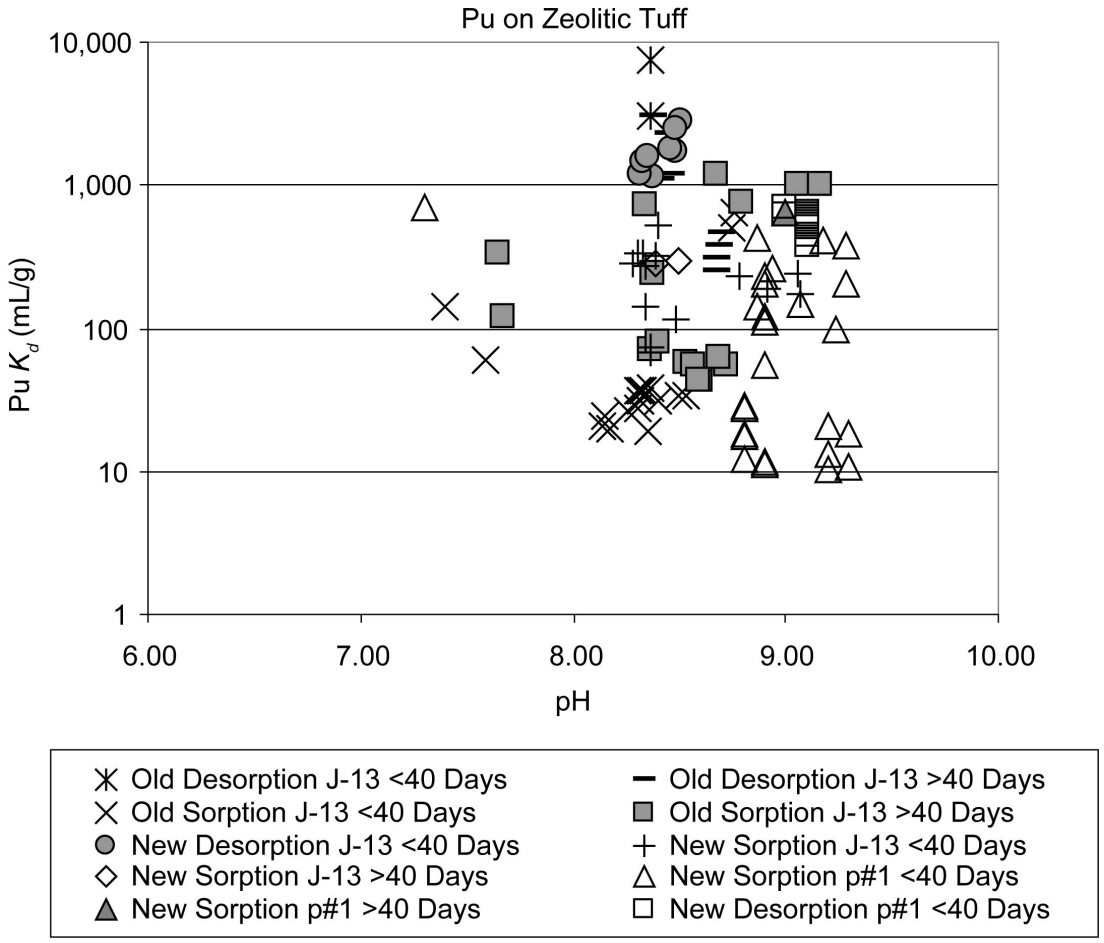

Sources: DTNs: LA0803AM831341.001 [DIRS 185573]; LA0809AM831341.003 [DIRS 185783].

NOTE: In the legend, 'old' stands for data collected before May 1989, 'new' stands for data collected after May 1989.

Figure A-28[b]. Plutonium Sorption Coefficients on Zeolitic Tuff in J-13 Well Water and Synthetic p#1 Water versus Solution pH in Sorption (Forward) and Desorption (Backward) Experiments

III.2.2.5 Corrections to Section A7.6.2, p. A-51

Figure A-35 is replaced by the following:

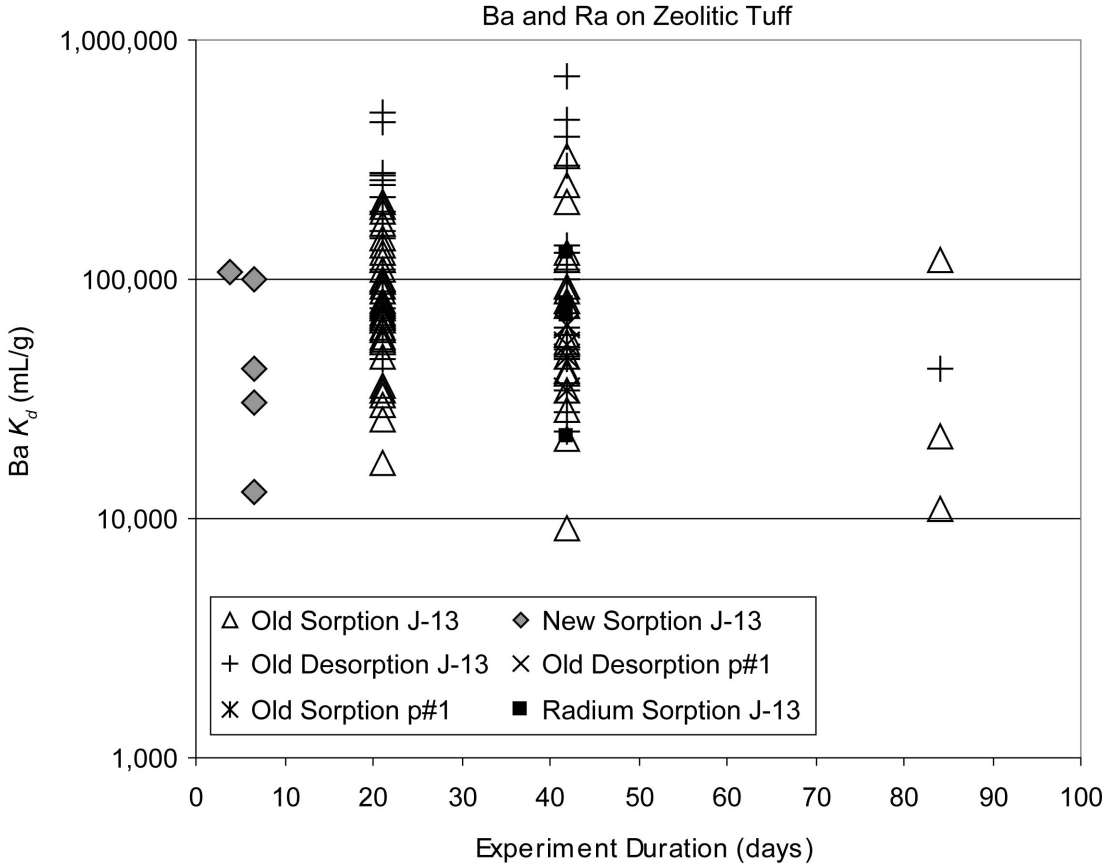

Sources: DTNs: LA0803AM831341.001 [DIRS 185573]; LA0407AM831341.001 [DIRS 170623].

NOTE: In the legend, 'old' stands for data collected before May 1989, 'new' stands for data collected after May 1989.

Figure A-35[b]. Barium and Radium Sorption Coefficients on Zeolitic Tuff in J-13 Well Water versus Experiment Duration for Sorption (Forward) and Desorption (Backward) Experiments

III.2.2.6 Corrections to Section A7.8.1, pp A-57 through A-60

Figures A-42, A-43, and A-44 are replaced by the following:

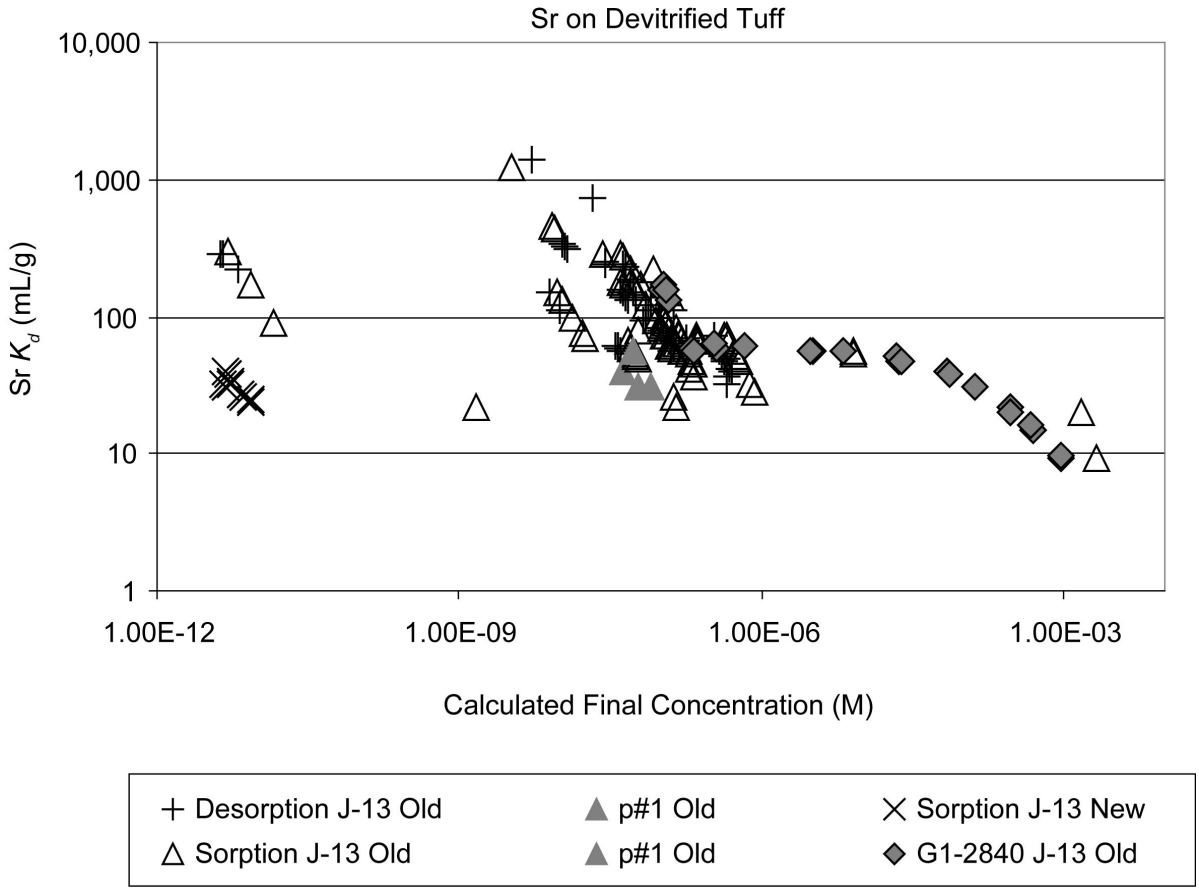

Source: DTNs: LA0803AM831341.001 [DIRS 185573]; LA0407AM831341.003 [DIRS 170626].

NOTE: In the legend, 'old' stands for data collected before May 1989, 'new' stands for data collected after May 1989.

Figure A-42[b]. Strontium Sorption Coefficients on Devitrified Tuff versus Calculated Final Strontium Concentration in Solution

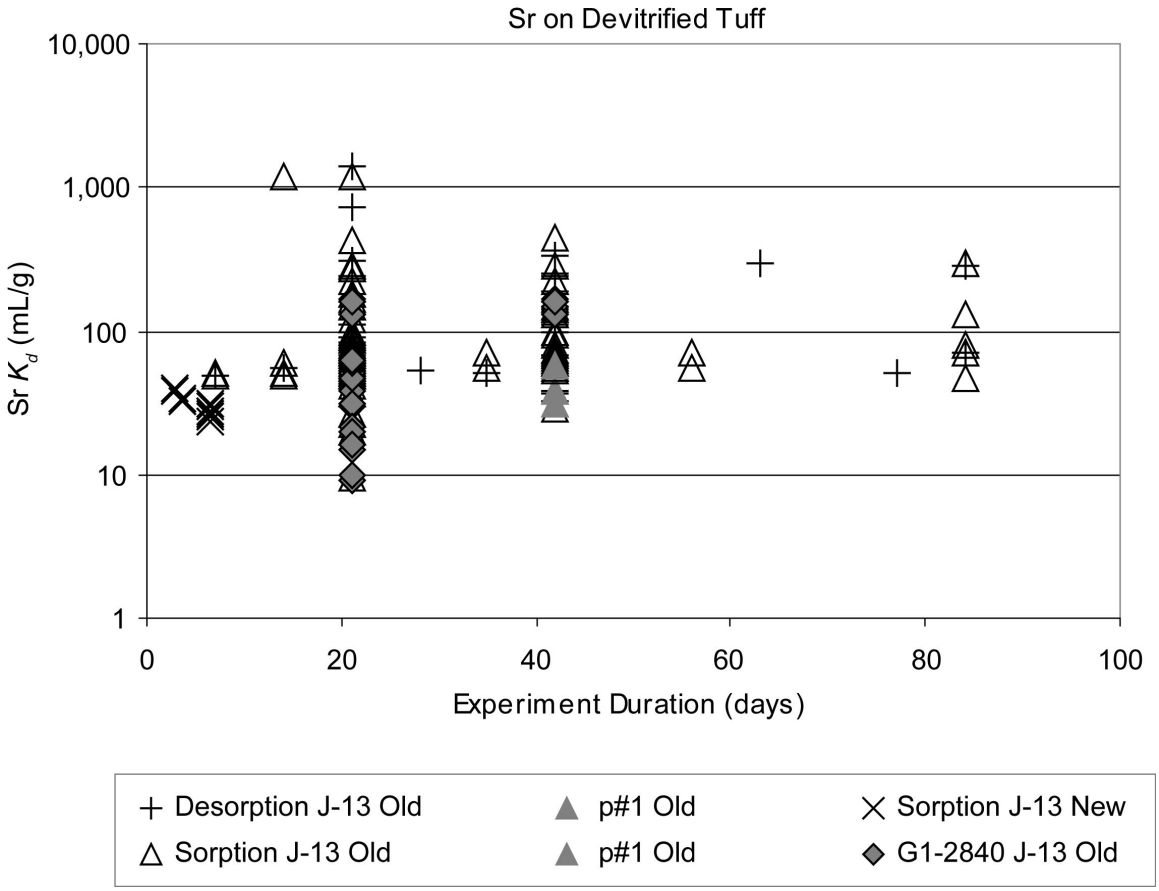

Source: DTNs: LA0803AM831341.001 [DIRS 185573]; LA0407AM831341.003 [DIRS 170626].

NOTE: In the legend, 'old' stands for data collected before May 1989, 'new' stands for data collected after May 1989. Data points include experiments in which fines were not removed from the samples.

Figure A-43[b]. Strontium Sorption Coefficients on Devitrified Tuff versus Experiment Duration for Sorption (Forward) and Desorption (Backward) Experiments

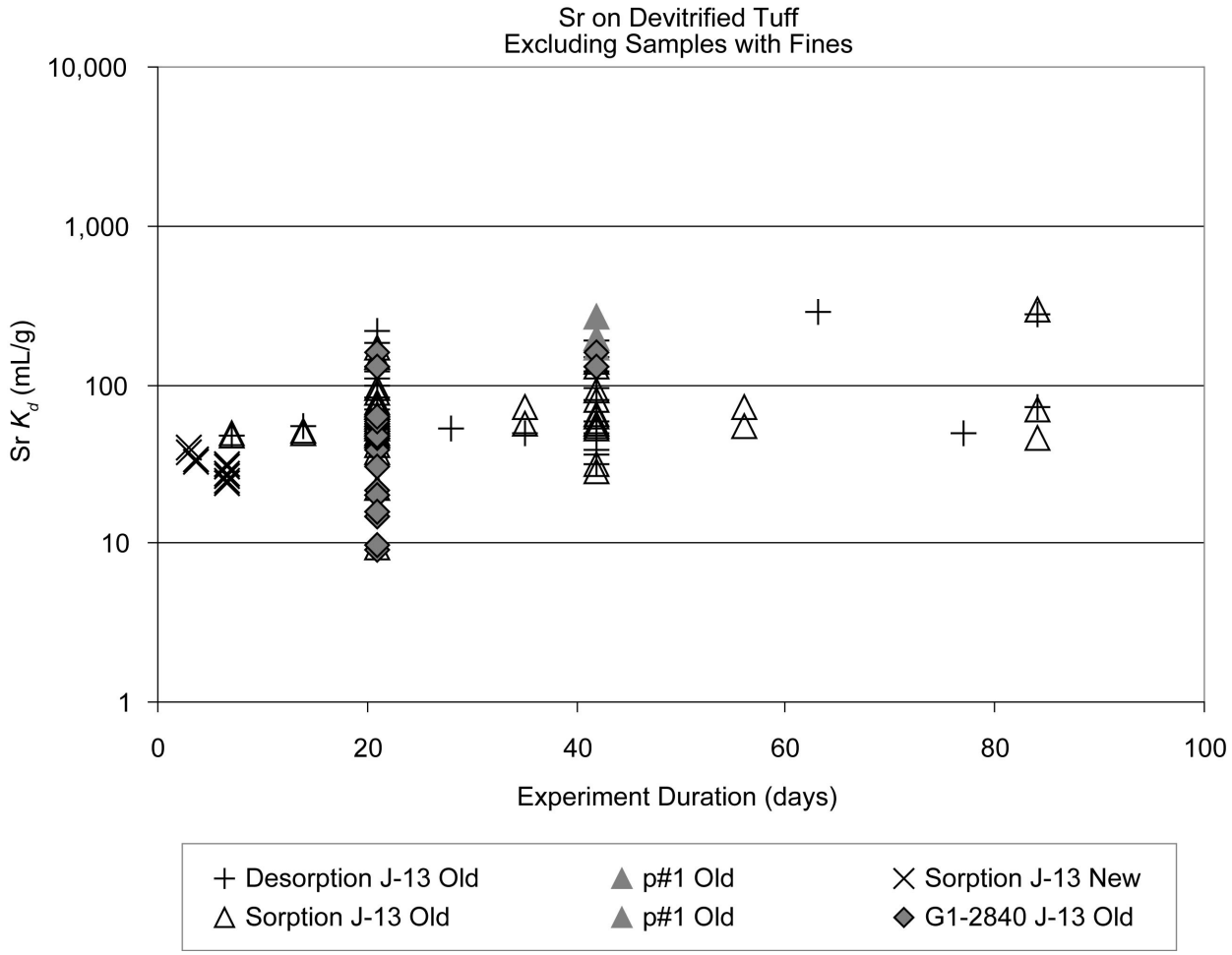

Source: DTNs: LA0803AM831341.001 [DIRS 185573]; LA0407AM831341.003 [DIRS 170626].

NOTE: In the legend, 'old' stands for data collected before May 1989, 'new' stands for data collected after May 1989. Samples containing fines fraction are removed from the figure.

Figure A-44[b]. Strontium Sorption Coefficients on Devitrified Tuff versus Experiment Duration for Sorption (Forward) and Desorption (Backward) Experiments with Reduced Range

III.2.2.7 Corrections to Section A7.9.1, pp. A-65 and A-66

Figures A-49 and A-50 are replaced by the following, **and** the following two paragraphs added to the Section A7.9.1:

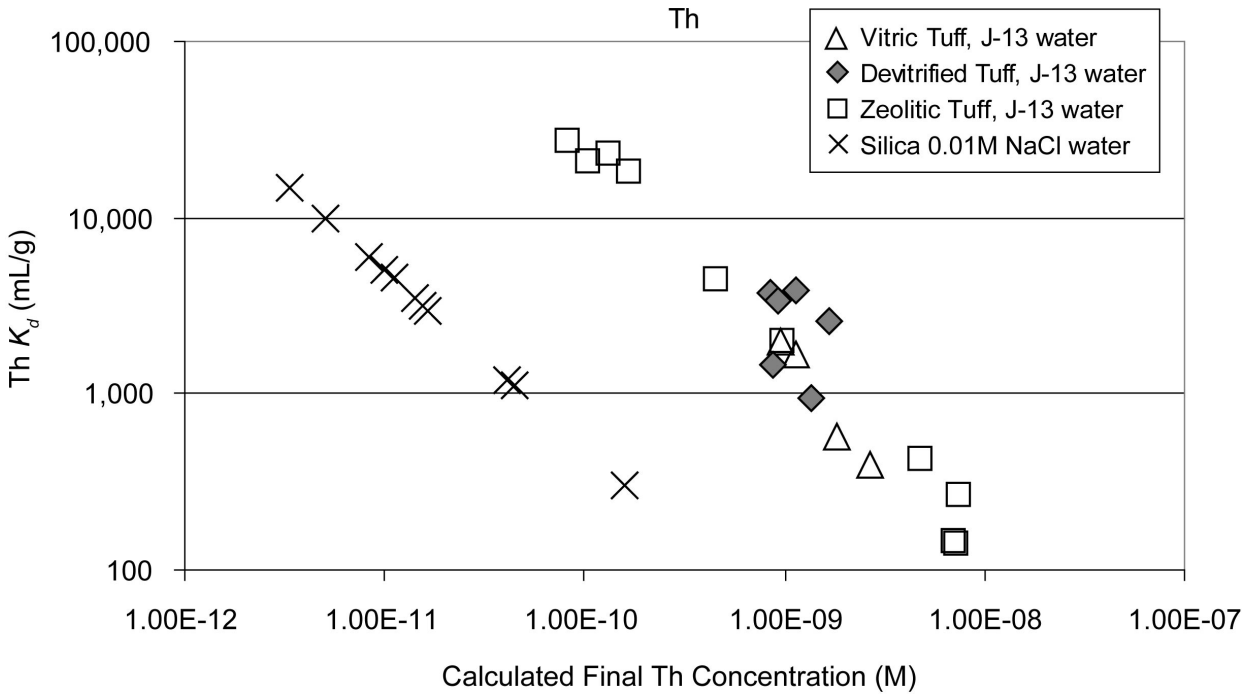

Source: DTN: LA0803AM831341.001 [DIRS 185573].

Figure A-49[b]. Thorium Sorption Coefficients on Tuff versus Calculated Final Thorium Concentration in Solution

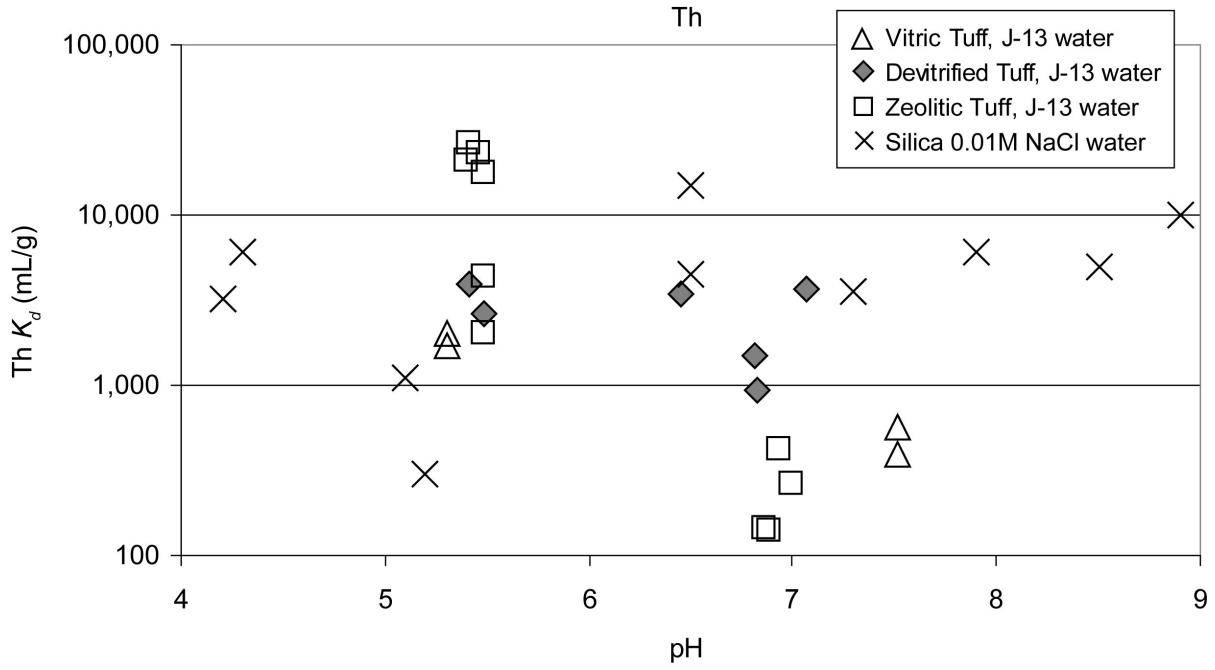

Source: DTN: LA0803AM831341.001 [DIRS 185573].

Figure A-50[b]. Thorium Sorption Coefficients on Tuff versus pH

The thorium K_d measurements for silica included in Figures A-49[b] and A-50[b] are documented in LA0803AM831341.001 [DIRS 185573]. Comparison of these silica K_d values to tuff measurements is reasonable because tuffs contain up to 76 wt % silica (Broxton et al. 1986 [DIRS 100023], p. 39). The surface area of the silica particles in the experiments is 2.8 m^2/g. Specific surface area is not reported for the tuff samples of the thorium K_d measurements, but several measurements for similar tuff samples are provided in Table A-1. Their ranges are 1.8 to 6.4 m^2/g for seven devitrified tuff samples, 0.52 to 3.3 m^2/g for three vitric tuff samples, and 18 to 66 m^2/g for ten zeolitic tuff samples. Because K_d values are generally proportional to specific surface area, the silica K_d measurements plotted in Figures A-49[b] and A-50[b] provide a reasonable comparison to the K_d measurements for the vitric and devitrified tuff samples. The tuff measurements used J-13 water, but the silica measurements used a pH-adjusted 0.01 M $NaClO_4$ solution. As noted earlier in Section A7.9.1, water chemistry is expected to have very little influence on thorium sorption-coefficient values in Yucca Mountain groundwaters. Hence, it is reasonable to augment the K_d data for devitrified tuff, as shown in Figures A-49[b] and A-50[b], with the silica data documented in DTN: LA0803AM831341.001 [DIRS 185573].

In Figure A-49[b], it is seen that the K_d values for silica, and zeolitic tuff generally span the same range, from about 1000 mL/g (for experiments with concentrations below the solubility limit of ~3.2 X 10^{-9} M at pH>6, as noted in Section A7.9) to above 10,000 mL/g. The data for devitrified tuff fall within this range also, although these data, with only 6 points, are much more limited. It is noted that the SZ model averages the K_d values over much larger spatial extent compared to the unsaturated zone (MDL-NBS-HS-000008 ERD02 [DIRS 177396]) and thus the units designated as devitrified in the SZ are likely to encompass local regions with higher zeolitic content. Hence, it is justified to use the same uncertainty distributions in the SZ for thorium K_ds for both devitrified and zeolitic tuffs. For these reasons, the uncertainty distributions for thorium K_ds in the SZ are not modified, in contrast to the treatment in the unsaturated zone (MDL-NBS-HS-000008 ERD02 [DIRS 177396]).

III.2.2.8 Corrections to Sections A7.11.1 and A7.11.2, pp. A-69 through A-77

Figures A-53 through A-60 replaced by the following:

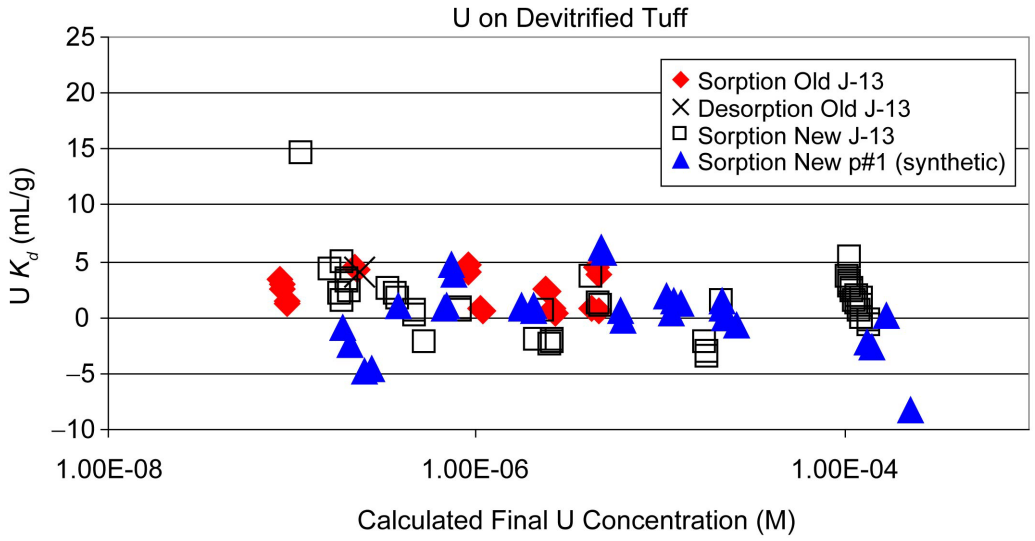

Source: DTNs: LA0803AM831341.001 [DIRS 185573]; LA0407AM831341.006 [DIRS 170628].

NOTE: In the legend, 'old' stands for data from before PVAR, 'new' stands for after PVAR data.

Figure A-53[b]. Uranium Sorption Coefficients on Devitrified Tuff versus Calculated Final Uranium Concentration in Solution

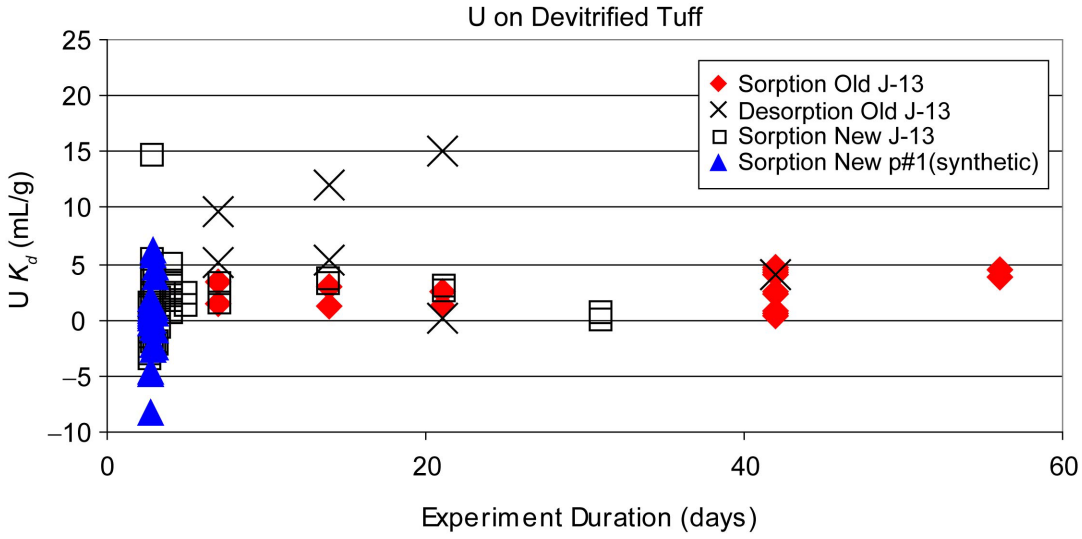

Source: DTNs: LA0803AM831341.001 [DIRS 185573]; LA0407AM831341.006 [DIRS 170628].

NOTE: In the legend, 'old' stands for data collected before May 1989, 'new' stands for data collected after May 1989.

Figure A-54[b]. Uranium Sorption Coefficients on Devitrified Tuff versus Experiment Duration for Sorption (Forward) and Desorption (Backward) Experiments

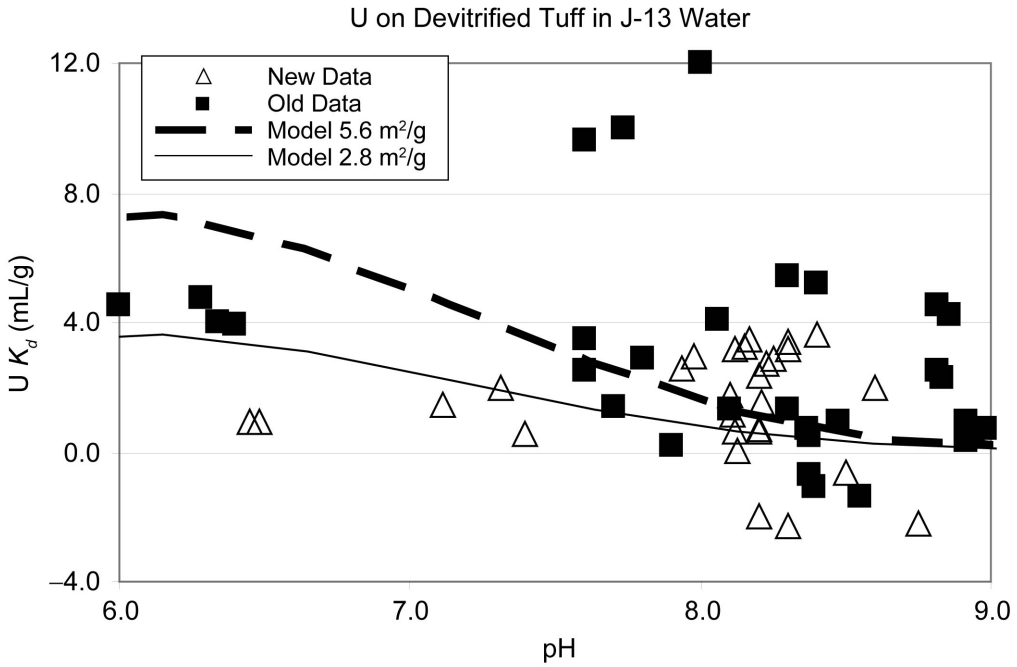

Source: DTNs: LA0803AM831341.001 [DIRS 185573]; LA0407AM831341.006 [DIRS 170628].

NOTE: In the legend, 'old' stands for data collected before May 1989, 'new' stands for data collected after May 1989. Model curves are from the PHREEQC surface-complexation model (Output DTN: LA0702MD831232.002, file *output_07.xls*, worksheets *Udtj13.pun.xls* and *Udt2j13.pun.xls*).

Figure A-55[b]. Uranium Sorption Coefficients on Devitrified Tuff versus pH

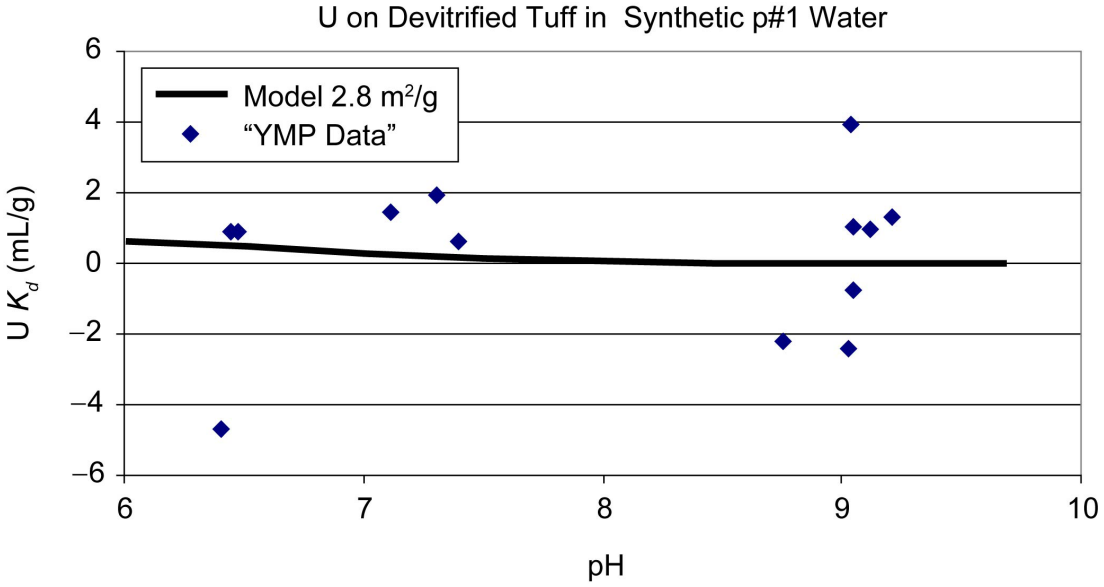

Source: DTNs: LA0803AM831341.001 [DIRS 185573]; LA0407AM831341.006 [DIRS 170628].

NOTE: Model curve is from the PHREEQC surface-complexation model (Output DTN: LA0702MD831232.002, file *output_07.xls*, worksheet *Udtp1.pun.xls*).

Figure A-56[b]. Uranium Sorption Coefficients on Devitrified Tuff in Synthetic p#1 Water versus pH

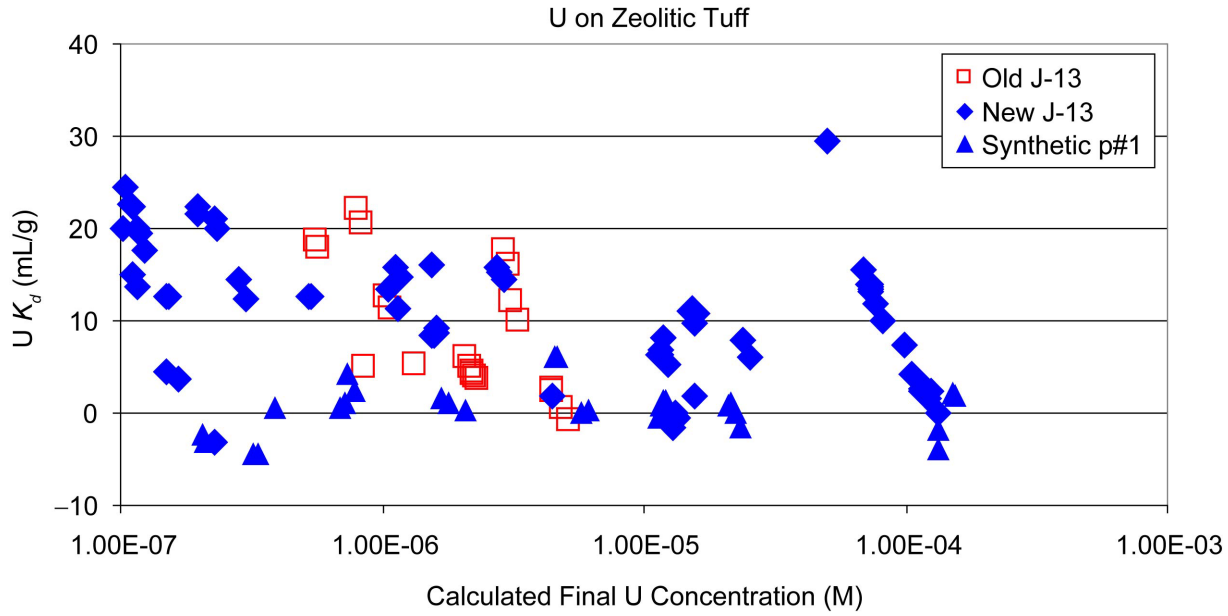

Source: DTNs: LA0803AM831341.001 [DIRS 185573]; LA0407AM831341.006 [DIRS 170628].

NOTE : In the legend, 'old' stands for data collected before May 1989, 'new' stands for data collected after May 1989.

Figure A-57[b]. Uranium Sorption Coefficients on Zeolitic Tuff versus Calculated Final Uranium Concentration in Solution

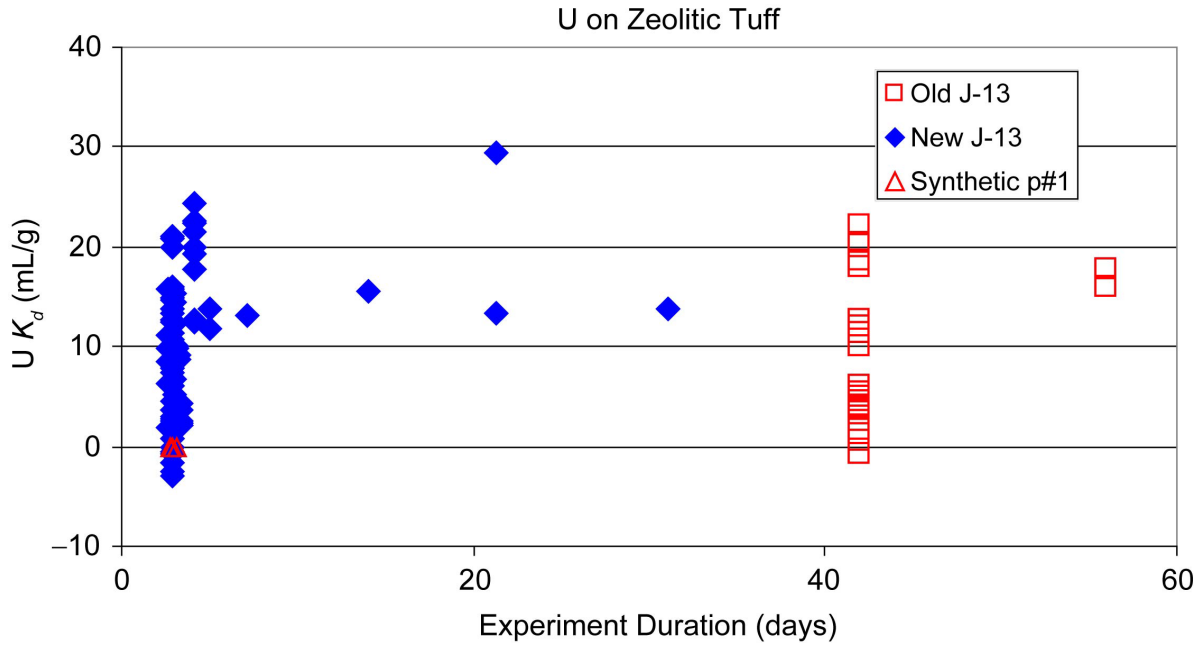

Source: DTNs: LA0803AM831341.001 [DIRS 185573]; LA0407AM831341.006 [DIRS 170628].

NOTE: In the legend, 'old' stands for data before PVAR, 'new' stands for after PVAR data.

Figure A-58[b]. Uranium Sorption Coefficients on Zeolitic Tuff as a Function of Experiment Duration

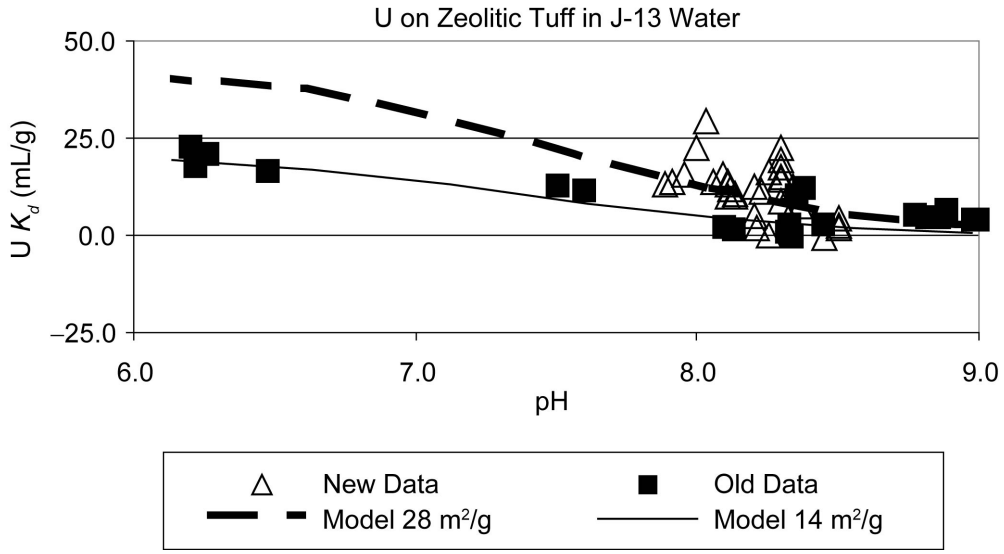

Source: DTNs: LA0803AM831341.001 [DIRS 185573]; LA0407AM831341.006 [DIRS 170628].

NOTE: In the legend, 'old' stands for data collected before May 1989, 'new' stands for data collected after May 1989. Model curves derived with PHREEQC surface-complexation modeling are also shown (Output DTN: LA0702MD831232.002, file *output _07.xls*, worksheets *Uzeolitj13.pun.xls and Uzeolj13.pun.xls*).

Figure A-59[b]. Uranium Sorption Coefficients for Zeolitic Tuff in J-13 Well Water Plotted as a Function of pH

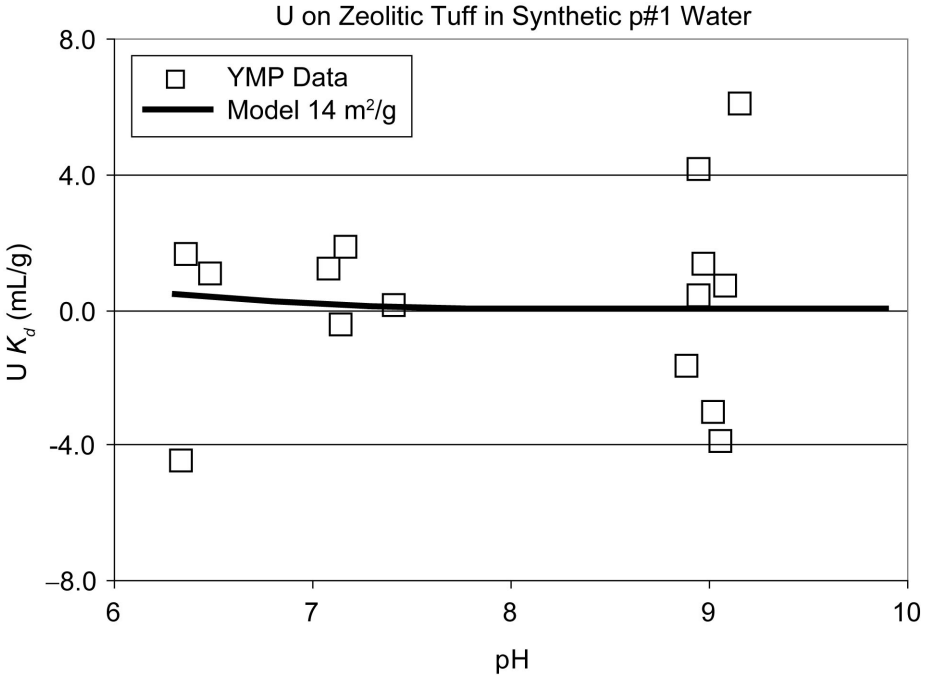

Source: DTNs: LA0803AM831341.001 [DIRS 185573]; LA0407AM831341.006 [DIRS 170628].

NOTE: Model curves derived with PHREEQC surface-complexation modeling are also shown (Output DTN: LA0702MD831232.002, file *output_07.xls*, worksheet *Uzeop1.pun.xls*).

Figure A-60[b]. Uranium Sorption Coefficients for Zeolitic Tuff in Synthetic p#1 Water as a Function of pH

III.2.2.9 Corrections to APPENDIX H

III.2.2.9.1 Corrections to Section H1

Section H1 is replaced by the following:

The qualification of 1977 to 1987 sorption measurements of Am, Ba, Cs, Np, Pu, Pa, Sr, Th, and U with Yucca Mountain tuff samples from DTN: LA0803AM831341.001 is documented here in accordance with SCI-PRO-001, *Qualification of Unqualified Data*. This qualification provides a desired level of confidence that the data are suitable for their intended use, which is limited to the subject of this work product (SZ radionuclide transport) for use in total system performance assessment (TSPA). The qualification is based on corroboration of data and technical assessment. The plan for the qualification of this data is presented at the end of this appendix.

III.2.2.9.2 Corrections to Section H1.1

The Section H1.1 is replaced by the following:

One important aspect of the data qualification process is corroboration of unqualified data with qualified data. If it can be shown that unqualified sorption coefficient experiments on a given water/rock combination and under a specified set of experimental parameters produced sorption coefficient data that are equivalent to data obtained under a qualified quality assurance (QA) program using a similar set of rock/water combinations and experimental parameters, the concordance of the two data sets can be used to support the qualification of the unqualified data set.

Sorption coefficients are subject to a range of factors including some associated with the solid phase, some associated with the liquid phase (groundwater or pore water), and some associated with the element-of-interest. The two main factors associated with the solid phase include mineralogy and surface area. Mineralogy includes mineral type and mineral composition, particularly for minerals that sorb primarily by ion exchange. The factors in the liquid phase that can influence sorption behavior are different for different elements-of-interest. For example, for alkali and alkaline earth elements of interest (i.e., barium, cesium, strontium, and radium), the concentrations of alkali and alkali earth elements in solution (e.g., calcium, phosphorus, sodium, and magnesium) are important factors. For an element such as uranium, pH, and alkalinity are important factors. Factors associated with the element-of-interest include concentration in solution and complexation behavior.

In comparing an unqualified dataset with a qualified dataset for a given element-of-interest, it is important that the factors that can control sorption behavior are at the same or similar values in both datasets unless it can be shown that a given factor does not control sorption behavior for the element-of-interest.

Two examples are cited of comparisons of qualified and unqualified datasets for elements-of-interest, the first is barium representing radionuclides that sorb by ion exchange and the second is uranium representing radionuclides that sorb by surface complexation. The first example is for barium sorption coefficients on zeolitic tuff in J-13 well water. Qualified and unqualified data points for sorption coefficients and final solution concentrations are shown in Figure H-1[b].

The same water composition was used in both the unqualified and the qualified experiments. Thus, differences in water composition are not an issue in comparisons of the two datasets. The differences in final solution concentrations did not influence the sorption coefficient ranges for the two datasets because the isotherms for barium sorption on zeolitic tuff in J-13 well water are essentially linear as shown in Figure A-34. Differences in experimental duration did not influence the sorption coefficient ranges because the barium sorption reactions are fast, as discussed in Section A7.6.2. The fact that the qualified data fall within the range of sorption coefficient values of the data to be qualified, and the majority of the data to be qualified falls within the range of values of the qualified data provides confidence that the experimental procedures used to obtain the unqualified data were appropriate and equivalent to those used to obtain the qualified dataset.

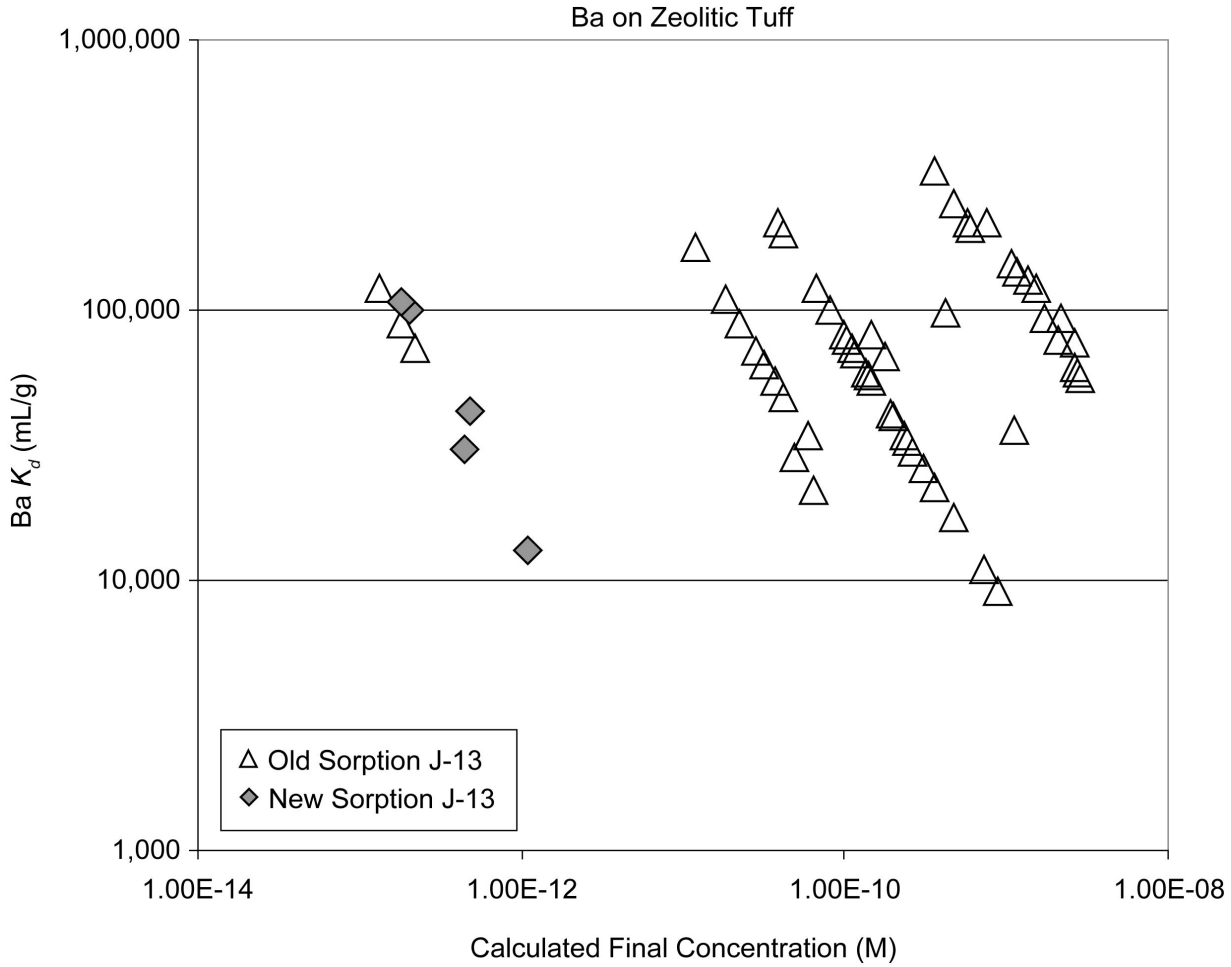

Source: DTNs: LA0803AM831341.001 [DIRS 185573]; and LA0407AM831341.001 [DIRS 170623] (corroborating data).

NOTE: In the legend, 'old' stands for data before PVAR, 'new' stands for data after PVAR.

Figure H-1[b]. Barium Sorption Coefficient on Zeolitic Tuff in J-13 Well Water versus Calculated Final ^{133}Ba Solution Concentration

The second example of a comparison of qualified and unqualified datasets involves uranium sorption on devitrified tuff in J-13 well water. Qualified and unqualified data points for sorption coefficients and pH are shown in Figure H-2[b]. The same water composition was used in both the unqualified and the qualified experiments. Thus, differences in water composition are not an issue in comparisons of the two datasets. The differences in final solution concentrations did not influence the sorption coefficient ranges for the two datasets because the uranium sorption coefficients are not sensitive to final solution concentrations as shown in Figure A-53[b].

Differences in experimental duration did not influence the sorption coefficient ranges because the uranium sorption reactions on devitrified tuff are fast, as discussed in Section A7.9.1. The fact that the ranges in uranium sorption coefficient values are similar for the two datasets, excluding the few outliers with a $K_d \geq 10$ mL/g, provides confidence that the experimental procedures used to obtain the unqualified data were appropriate and equivalent to those used to obtain the qualified dataset.

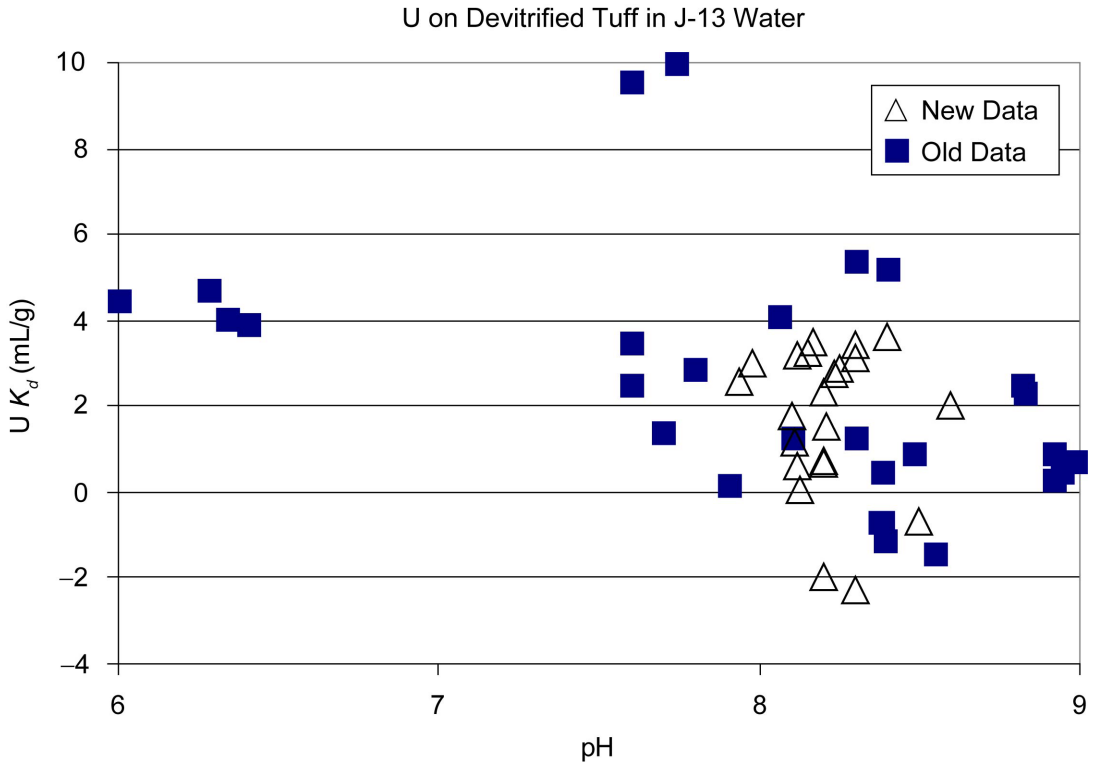

Source: DTNs: LA0305AM831341.001 [DIRS 163789]; LA0407AM831341.006 [DIRS 170628] (corroborating data).
NOTE: In the legend, 'old' stands for data before PVAR, 'new' stands for data after PVAR.

Figure H-2[b]. Uranium Sorption Coefficient on Devitrified Tuff in J-13 Well Water versus pH

III.2.2.9.3 Corrections to Section H1.2

Section H1.2 is replaced by the following:

Technical assessment of the data being evaluated was performed by Arend Meijer, a member of the data qualification team, who is a recognized subject matter expert in the area of sorption coefficients. It was determined that the employed methodology for data collection was

acceptable because a) it followed a well-established quality assurance program at the Los Alamos National Laboratory (LANL) b) experiments were performed under work plans that were reviewed by a board, c)data were collected by properly trained professionals d) equipment calibration was controlled. These items are described below:

The LANL studies of the sorptive behavior of tuff and transport of radionuclides through tuff were performed under the Nevada Nuclear Waste Storage Investigations (NNWSI) project that was managed by the Nevada Operations Office of the DOE. These investigations were performed under the Los Alamos QA program for the NNWSI, with the Materials Science and Technology Division quality assurance organization responsible for the planning and implementation of the Los Alamos QA program. *Los Alamos National Laboratory Quality Assurance Plan And Procedures For The Nevada Nuclear Waste Storage Investigations* (LA-9331-MS) is a collection of the quality assurance documents that provides a detailed account of the Los Alamos NNWSI QA program, including the Quality Assurance Program Plan, the Quality Assurance Program Index and Procedures, work plans, and the detailed procedures developed for the Yucca Mountain Project (YMP).

The QA program developed for the NNWSI at Los Alamos was outlined in the Quality Assurance Program Plan and was structured to meet the requirements of NQA-1 and 10 CFR 50 ([DIRS 176567], Appendix B), as applied to the evaluation of major geologic formations with regard to their suitability as locations of permanent repositories for high-level radioactive wastes. *Quality Assurance Program Index* (TWS-QI-1 and TWS-CMBQA-QP-02) is a cross-reference between basic requirements standards NQA-1 and 10 CFR 50 [DIRS 176567] showing where these requirements are addressed in the Los Alamos Quality Assurance Manual (QAM) and YMP implementing procedures. The QAM was the primary compliance document for this work unless otherwise stated in the Quality Assurance Program Plan or in the specific procedure documents written for NNWSI.

Work plans were the primary planning documents covering the Los Alamos technical activities for the NNWSI. These work plans were written to provide an adequate description of the scope and purpose of the task. They include, directly or by reference, the QA requirements with regard to data validity and documentation. Review boards that consisted of, at a minimum, a management member, a QA member, and an independent technical reviewer who was experienced and competent in the field under review but had no direct program responsibility, approved the work plans as well as the acceptance of final documents. The work plan TWS-CNC-WP-03, *Tuff Experiments-Sorption Ratios and Migration Measurements* described the scope of work; provided an overview of how batch sorption studies were to be performed; defined which procedure to be used to control the experiments; and detailed performance, equipment, QA, and work documentation requirements for the radioactivity measurements. TWS-CNC-DP-05, *Sorption, Desorption Ratio Determinations of Geologic Materials by a Batch Method* was used to control the experiments in the same process as used in LANL-INC-DP-86, *Sorption and Desorption Determinations by a Batch Sample Technique for the Dynamic Transport Task* to control the qualified K_d data.

Training requirements for personnel were delineated in the QAM by QMR 1, *Quality Assurance Management and Planning* and QMI 1-1, *Quality Program Management*. Measuring and testing equipment that require calibration was controlled in accordance with the applicable sections of

the QAM (QMR 9 and QMI 9-1). The only equipment used for these experiments that required calibration were the balances and gamma counters. These were controlled in accordance with procedures QMR 9 *Control and Calibration of Standards and Measuring and Testing Equipment* and QMI 9-1 *Acquisition and Calibration Control of Standards and Measuring and Testing Equipment*. *Quality Assurance Audit of Los Alamos National Laboratories (LANL) Nevada Nuclear Waste Storage Investigations (NNWSI) Project* (LANL 1984 [DIRS 171444]) (performed July 16 through 18, 1984) verified that the control of measuring and test equipment was adequate. There were no problems found with the measuring and test equipment program. *Audit of Los Alamos Scientific Laboratories Quality Assurance Program Plan for Nevada Nuclear Waste Storage Investigations* (Los Alamos Scientific Laboratories 1979 [DIRS 171445]) (conducted May 1 to 3, 1979) also found that the measuring and test equipment program was satisfactory.

Corrective actions for significant conditions adverse to quality were provided in accordance with QMR 12, *Corrective Action,* of the QAM. Compliance with the QA program was verified by periodic audits that were planned, documented, and carried out in accordance with QMI 15-1, *Quality Audits,* of the QAM.

III.2.2.9.4 Corrections to Section H1.3

Section H1.3 is replaced by the following:

The programs in place at the time these sorption experiments were performed and the fact that the audits mentioned above did not identify anything that would affect the quality of the data lend support to the conclusion that the data collection methodology and equipment used were appropriate for the type of data under consideration. Corroborating information available for barium and uranium also show the equivalence of the unqualified and qualified data, supporting the adequacy of the unqualified data set. Furthermore, the uncertainty distributions for sorption coefficients generally span a range that is one order of magnitude or more (see Table C-14). The corroborating data comparisons suggest that differences between the unqualified and qualified data are much less than the inherent uncertainty. Therefore, the data are qualified for use in supporting the sorption coefficient distributions to be used in TSPA.

III.2.2.10 Corrections to Appendix L

Section L7 is added to qualify the Thorium sorption data on silica from Allard et al. 1983 [DIRS 162982], as follows:

L7. SORPTION COEFFICIENT DATA FOR THORIUM ON SILICA IN A SIMPLE ELECTROLYTE BY ALLARD ET AL. 1983 [DIRS 162982]

Data Qualification Methods: SCI-PRO-001, Attachment 3, Method 5.

Data Qualification Attributes: SCI-PRO-001, Attachment 4, Attributes 1, 3, and 8.

Discussion: The available data on site-specific sorption coefficients for thorium are very limited. The thorium sorption coefficient data presented by Allard et al. (1983 [DIRS 162982]) were published in a paper titled, “Sorption Behavior of Actinides in Well-defined Oxidation States,”

published by the Swedish Nuclear Fuel and Waste Management Company (SKB). The work of SKB is well respected in the international nuclear waste community. Dr Allard is a professor of Chemistry/Environmental Sciences at the Orebro University, Sweden; and a member of the Royal Swedish Academy of sciences, and has extensive background in radiochemistry and measurement of sorption coefficients on silicate rocks.

Decision: The thorium sorption coefficient data is deemed reliable and appropriate for use in modeling thorium sorption behavior in Yucca Mountain samples.

III.2.2.11 Corrections to Section 9.1

Add the following entry:

177396 SNL (Sandia National Laboratories) 2007. *Radionuclide Transport Models Under Ambient Conditions.* MDL-NBS-HS-000008 REV 02 ADD 01. Las Vegas, Nevada: Sandia National Laboratories. ACC: DOC.20050823.0003; DOC.20070718.0003; DOC.20070830.0005; LLR.20080324.0002.

III.2.2.12 Corrections to Section 9.3

Entries for four superseded DTNs: LA0305AM831341.001, LA0310AM831341.001, LA0407AM831341.005, and LA0802AM831341.001were deleted; entries for the corresponding superseding DTNs were added as follows:

185081 LA0802AM831341.002. SE(Selenium) and SN (Tin) Sorption On Yucca Mountain Rock Samples. Submittal date: 02/20/2008.

185573 LA0803AM831341.001. 1977 To 1987 Sorption Measurements Of Am, Ba, Cs, Np, Pu, Pa, Sr, Th, And U With Yucca Mountain Tuff Samples. Submittal date: 03/26/2008.

185783 LA0809AM831341.003. Batch Sorption Coefficient Data For Plutonium On Yucca Mountain Tuffs In Representative Water Compositions. Submittal date: 03/31/2008.

III.3 Analysis and Changes for CR 12300

III.3.1 Analysis

ANL-NBS-HS-000039 REV 02 [DIRS 177394] had two sections numbered 6.5.5. To correct this, the second section 6.5.5 of that document was renumbered as 6.5.6, and all following subsections within 6.5 were also incremented in response to CR 11731. The citations to that document were corrected as follows:

III.3.2 Changes to MDL-NBS-HS-000010 REV 03 AD 01

- p. 6-2, halfway down page, citation to DIRS 177394, Section 6.5.6 was changed to Section 6.5.7. Laboratory column transport experiments in Yucca Mountain alluvium

have indicated that sorption should be included in the alluvium transport model *Saturated Zone In-Situ Testing* (SNL 2007 [DIRS 177394], Section 6.5.7).

- p. 7-20, 4th line from bottom, citation to DIRS 177394, Section G5.4.3 was changed to Section G5.4.4. Field testing using single-well and cross-well tracer tests have confirmed the occurrence of sorption in alluvium downgradient of Yucca Mountain (SNL 2007 [DIRS 177394], Section 6.5.5 and Appendix G5.4.4).

III.4 Analysis and Changes for TBV-8234

III.4.1 Analysis

DTN: LA0702AM831341.001 [DIRS 179306] was superseded by DTN: LA0802AM831341.002 [DIRS 185081] to revise two data values attributed to transcription error and to revise the rock type classification of the samples G1-2233, G1-2289, G1-3116, G2-0547, GU3-1531, and GU3-433. The entries corresponding to DTN: LA0702AM831341.001 [DIRS 179306] in Table 4-1[a] and Section 9 of MDL-NBS-HS-000010 REV 03 AD 01 were changed. Figures A-36, A-37, A-39, and A-40 in MDL-NBS-HS-000010 REV 03 AD 01 were replaced.

III.4.2 Changes to MDL-NBS-HS-000010 REV 03 AD 01

III.4.2.1 Changes to Table 4-1

The entries corresponding to DTN: LA0702AM831341.001 [DIRS: 179306] in Table 4-1 were replaced with entries from the superseding DTN: LA0802AM831341.002 [DIRS 185081], as given in Section III.1.2.1.

III.4.2.2 Changes to Section 9

The following correction was made in Section 9 of MDL-NBS-HS-000010 REV 03 AD 01: Entry for DTN: LA0702AM831341.001[DIRS179306] was replaced with that for DTN: LA0802AM831341.002 [DIRS 185081] as follows:

185081 LA0802AM831341.002. SE(Selenium) and SN (Tin) Sorption On Yucca Mountain Rock Samples. Submittal date: 02/20/2008.

III.4.2.3 Changes to Section A7.7

The discussion in Section A7.7.1 of MDL-NBS-HS-000010 REV 03 AD 01 was modified and Figures A-36 and A-37 were replaced. Also, the discussion in Section A7.7.2 was modified and Figures A-39 and A-40 were replaced. The following subsections show the corrected text and figures:

III.4.2.3.1 Changes to Section A7.7.1, pp. A-52 and A-53

Figures A-36 and A-37, and the first two paragraphs of Section A7.7.1 are replaced by the following:

The experimentally derived sorption coefficients for selenium on devitrified tuff are plotted against the calculated final selenium concentrations of the experiments in Figure A-36[b]. These data were all obtained prior to May 1989. The range of K_d values obtained in sorption experiments was 1.4 to 34.1 mL/g. The range of K_d values obtained in desorption experiments was 20.0 to 93.6. The K_d values obtained in sorption experiments do not show a clear correlation with final solution concentration (Figure A-36[b]). In the case of K_d values obtained from desorption experiments, there is greater scatter in the data but also no clear correlation.

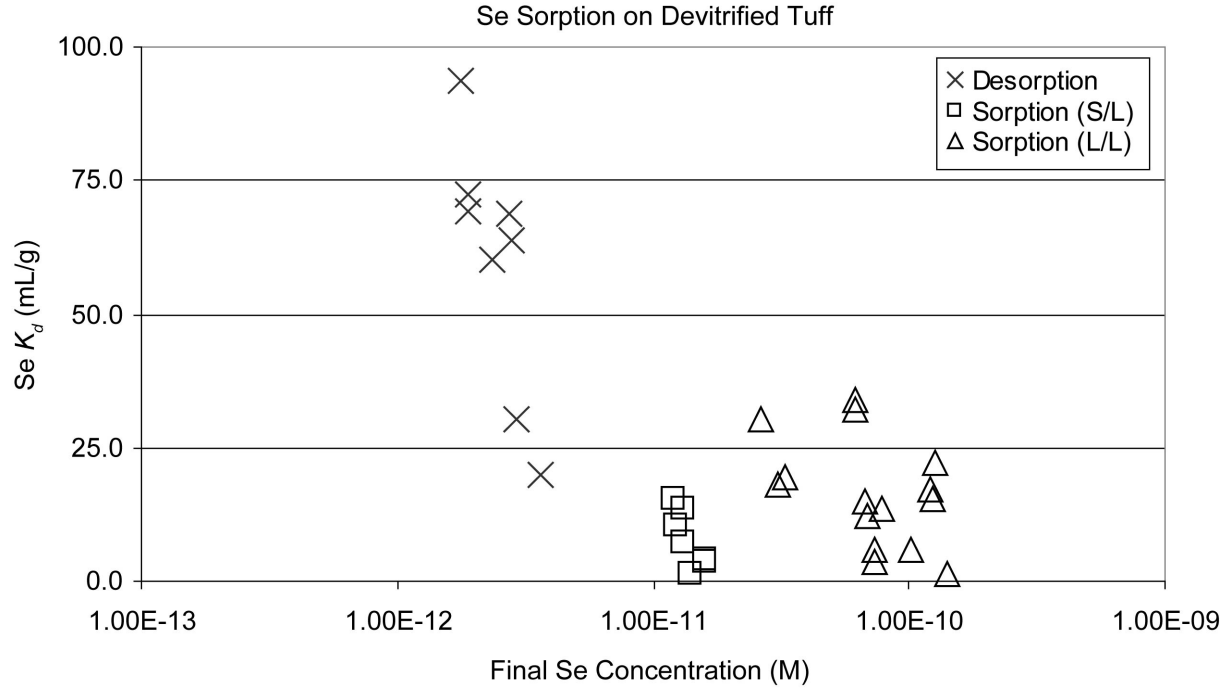

Source: DTN: LA0802AM831341.002 [DIRS 185081].

NOTE: S/L = Solid/Liquid, L/L = Liquid/Liquid (see text).

Figure A-36[b]. Selenium Sorption Coefficients on Devitrified Tuff versus Calculated Final Selenium Concentration in Solution

The equilibration rate for selenium sorption reactions on tuff can potentially be gauged from a plot of sorption coefficients versus experiment duration as shown in Figure A-37[b]. The normal expectation would be that for experiments of a given duration, K_d values from sorption experiments would be larger than those obtained from desorption experiments and would show an increase with experiment duration (i.e., a positive trend in Figure A-37[b]). The opposite would be expected for K_d values obtained from desorption experiments (negative trend in Figure A-37[b]). Unfortunately, there is too much scatter in the dataset to discern clear trends. However, the fact that K_ds obtained in desorption experiments are consistently larger in value than the K_ds obtained in sorption experiments is significant. It suggests that desorption rates are slow relative to sorption rates.

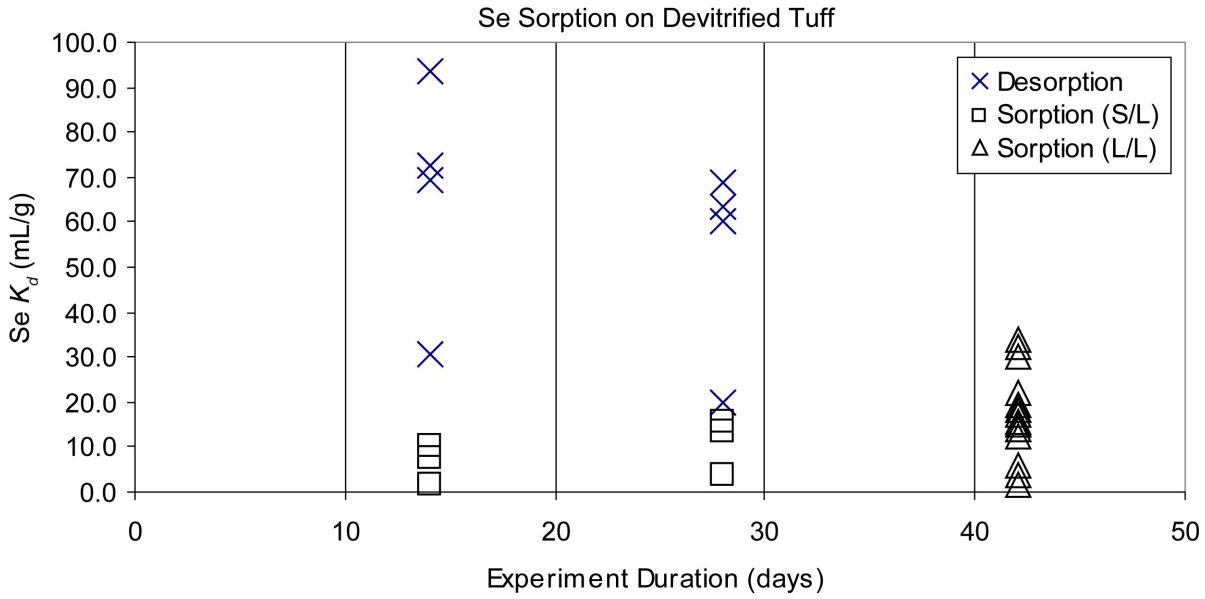

Source: DTN: LA0802AM831341.002 [DIRS 185081].

NOTE: S/L = Solid/Liquid, L/L = Liquid/Liquid (see text). Duration for sorption (forward) and desorption (backward) experiments.

Figure A-37[b]. Selenium Sorption Coefficients on Devitrified Tuff versus Experiment

Although data from the superseding DTN, plotted in Figure A-37[b], are different from those plotted in the previous version of the figure, the text explaining Figure A-37[b] remains valid. The K_d distribution remains unchanged

III.4.2.3.2 Changes to Section A7.7.2, pp. A-54 through A-56

Figures A-39 and A-40, and the first paragraph of Section A7.7.2 are replaced by the following:

The experimentally derived sorption coefficients for selenium on zeolitic tuff are plotted against the calculated final selenium concentrations of the experiments in Figure A-39[b], and versus experiment duration in Figure A-40[b]. These data were all obtained prior to May 1989. The range of K_d values obtained in sorption experiments in J-13 waters was from 1.3 to 51 mL/g. The range of K_d values obtained in the longer term (28 days) desorption experiments was 21.5 to 72.3. The K_d values obtained in sorption experiments do not show a clear correlation with final solution concentration. In the case of K_d values obtained from desorption experiments, there is greater scatter in the data but also no clear correlation. The equilibration rate for selenium sorption reactions on tuff can potentially be gauged from the plot of sorption coefficients versus experiment duration shown in Figure A-40[b]. As with selenium sorption on devitrified tuff, there is too much scatter in the dataset to discern clear trends. However, the fact that K_ds obtained in desorption experiments are consistently larger in value than the K_ds obtained in sorption experiments is significant. It suggests desorption rates are slow relative to sorption rates.

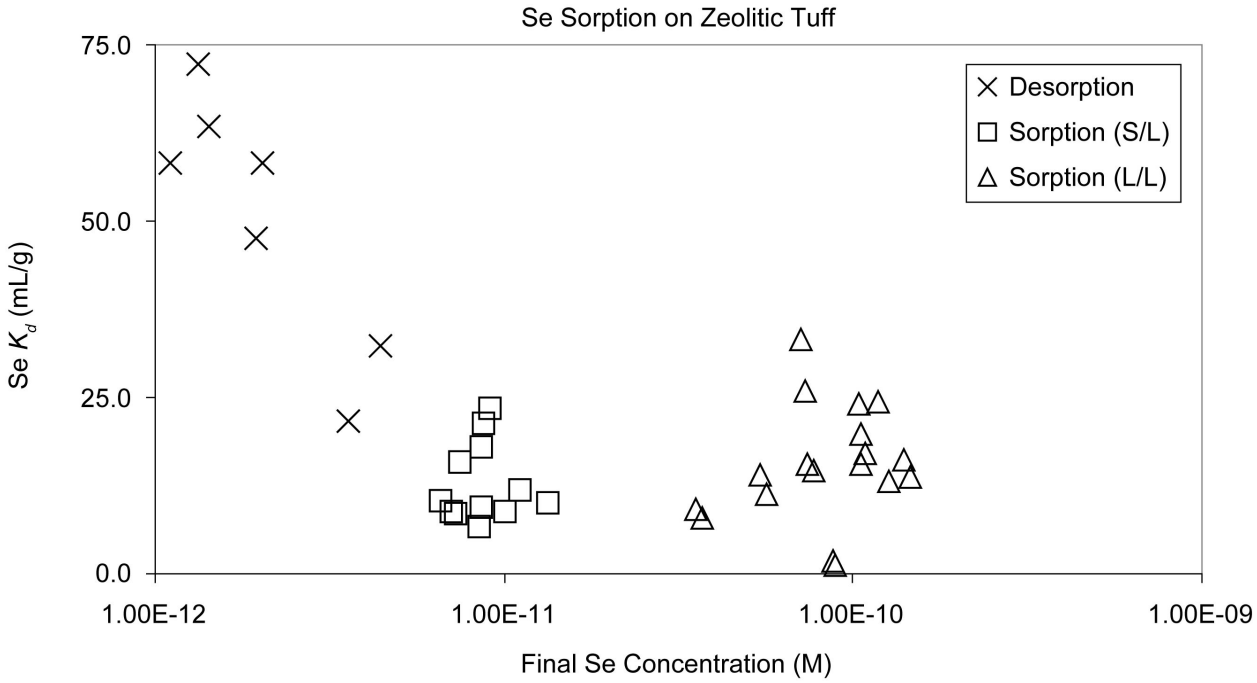

Source: DTN: LA0802AM831341.002 [DIRS 185081].

NOTE: S/L = Solid/Liquid, L/L = Liquid/Liquid (see text).

Figure A-39[b]. Selenium Sorption Coefficients on Zeolitic Tuff versus Calculated Final Selenium Concentration in Solution

Although data from the superseding DTN, plotted in Figure A-39[b], are different from those plotted in Figure A-39, the text explaining Figure A-39 remains valid for Figure A-39[b]. The K_d distribution remains unchanged.

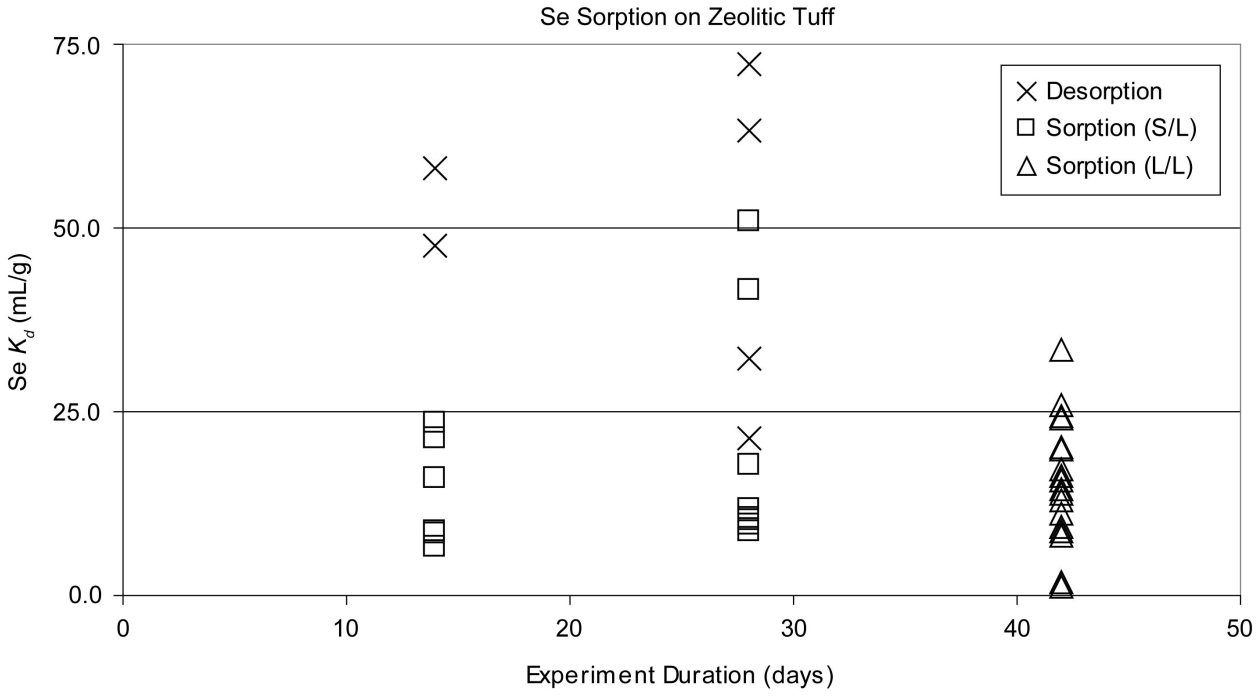

Source: DTN: LA0802AM831341.002 [DIRS 185081].

NOTE: S/L = Solid/Liquid, L/L = Liquid/Liquid (see text).

Figure A-40[b]. Selenium Sorption Coefficients on Zeolitic Tuff versus Experiment Duration for Sorption (Forward) and Desorption (Backward) Experiments

IV Impact Analysis

IV.1 Resolution of CR 11825

The corrections described in Section III.1.2, implemented in order to address CR 11825, do not affect the conclusions or output of MDL-NBS-HS-000010 REV 03 AD 01.

IV.2 Resolution of CR 11020 and CR 12647

The corrections described in Section III.2, implemented in order to address CR 11020 and CR 12647, do not affect the conclusions or output of MDL-NBS-HS-000010 REV 03 AD 01.

IV.3 Resolution of CR 12300

The corrections described in Section III.3 to address CR 12300 do not affect the conclusions or output of MDL-NBS-HS-000010 REV 03 AD 01.

IV.4 Resolution of CR 12360

The corrections provided in Attachment A to address CR 12360 do not affect the conclusions or output of MDL-NBS-HS-000010 REV 03 AD 01.

IV.5 Resolution of TBV-8234

The corrections described in Section III.4 to address TBV-8234 do not affect the conclusions or output of MDL-NBS-HS-000010 REV 03 AD 01.

IV.6 Changes to DIRS

1. Entry for DTN: LA0305AM831341.001 [DIRS 163789]: change to LA0803AM831341.001 [DIRS 185573]. For this entry change Submittal date to 03/26/2008. Change the DIRS # for this entry to 185573. Change the entry for 'Specifically Used From' to 'file LA0803AM831341-001 10Jun-08.xls'

2. Entry for DTN: MO0101XRDDRILC.002 [DIRS 163795], Change the entry for 'Specifically Used From' to 'Tables S01026_001 and S01026_002'

3. Entry for DTN: MO0101XRDMINAB.001 [DIRS 163796], Change the entry for 'Specifically Used From' to 'Tables S01023_002, S01023_003, S01023_004, and S01023_005'

4. Entry for DTN: MO0106XRDDRILC.003 [DIRS 163797], Change the entry for 'Specifically Used From' to 'Table S01074_001'

5. Delete the entry for DTN LA0310AM831341.001 [DIRS 165865]

6. Entry for DTN: LA0407AM831341.005 [DIRS 170625] change to DTN LA0809AM831341.003 [DIRS 185783]. For this entry, change 'Submittal Data" to 03/31/2008'. For this entry, change DIRS # to 185783.

7. Entry for DTN: LA0702AM831341.001 [DIRS 179306] change to LA0802AM831341.002 [DIRS 185081]. For this entry, change 'Submittal Date' to 02/20/2008. For this entry, change DIRS # to 185081

8. Entry for DTN: LAJC831321AQ98.005 [DIRS 109004]: Change the entry for 'Specifically Used From' to 'Tables S98436_001, S98436_002, S98436_003, and S98436_004".

9. Entry for DTN: MO0408K8313211.000 [DIRS 171437]: Change the entry for 'Specifically Used From' to 'Table S04337_001".

10. Add new entry for SNL (Sandia National Laboratories) 2007. [DIRS 177396]: Radionuclide Transport Models Under Ambient Conditions. MDL-NBS-HS-000008 REV 02 ADD 01. Las Vegas, Nevada: Sandia National Laboratories. ACC: DOC.20050823.0003; DOC.20070718.0003; DOC.20070830.0005; LLR.20080324.0002.

11. Entry for [DIRS 145195]: add used in Section 6.4.2.2, Used From Equations A1, Description:" dispersion tensor and displacement matrix"

12. Entry for [DIRS 145195]: add used in Section 6.4.2.3, Equation 20, Used From Equations A13a, A13b, and A11.

13. Entry for [DIRS 163821]: Delete section 2.6 in 'used from'. Delete Equation 66 in 'used from'.

IV.7 Impact on Downstream Users

The updates to the parent report described in this ERD have not modified the conclusions and technical product outputs of the MDL-NBS-HS-000010 REV 03 AD 01. The documents listed as "controlled" and "under development" in the DIRS Impact Analysis for MDL-NBS-HS-000010 REV 03 and MDL-NBS-HS-000010 REV 03 AD 01 were checked for impact. The only document that is impacted is the LA Safety Analysis Report (DOE/RW-0573 REV0, Section 2.3.9). Figures 2.3.9-29, 2.3.9-30, 2.3.9-31, and 2.3.9-32 of the LA Safety Analysis Report must be replaced respectively by Figures A-23[b], A-27[b], A-54[b] and A-58[b] from this ERD. The documents checked for impact are listed below:

- *Postclosure Nuclear Safety Design Bases* (ANL-WIS-MD-000024 REV 01)
- *Features, Events, and Processes for the Total System Performance Assessment: Analyses* (ANL-WIS-MD-000027 REV 00)
- *Total System Performance Assessment Model/Analysis for the License Application* (MDL-WIS-PA-000005 REV 00 AD 01)
- *Data Qualification Report for Selenium and Tin Sorption Data Obtained by Los Alamos National Laboratory, 1981 to 1984* (TDR-CRW-HS-000001 REV 00)
- *Saturated Zone In-Situ Testing* (ANL-NBS-HS-000039 REV 02)
- *Waste Form and In-Drift Colloids-Associated Radionuclide Concentrations: Abstraction and Summary* (MDL-EBS-PA-000004 REV 03)
- *UZ Flow Models and Submodels* (MDL-NBS-HS-000006 REV 03)
- *Radionuclide Transport Models Under Ambient Conditions* (MDL-NBS-HS-000008 REV 02, ACN 02, AD 01)
- *Saturated Zone Site-Scale Flow Model* (MDL-NBS-HS-000011 REV 03)
- *Saturated Zone Flow and Transport Model Abstraction* (MDL-NBS-HS-000021 REV 03 AD 01)
- *Saturated Zone Flow and Transport Model Abstraction* (MDL-NBS-HS-000021 REV 03, AD 02)

- *Total System Performance Assessment Model/Analysis for the License Application* (MDL-WIS-PA-000005 REV 00, MiscId 01, MiscId 02, MiscId 03, and MiscId 11)

- *TSPA Information Package for the Draft Supplemental Environmental Impact Statement* (TDR-WIS-PA-000014 REV 00)

- LA Safety Analysis Report, Section 2.3.9 ((DOE/RW-0573 REV0).

Data Qualification Plan

Complete only applicable items.

QA: QA
Page 1 of 1

Section I. Organizational Information

Qualification Title
Qualification of sorption data, DTN: LA0803AM831341.001

Requesting Organization
LANL

Section II. Process Planning Requirements

1. List of Unqualified Data to be Evaluated

1977 TO 1987 SORPTION MEASUREMENTS OF AM, BA, CS, NP, PU, PA, SR, TH, AND U WITH YUCCA MOUNTAIN TUFF SAMPLES (DTN LA0803AM831341.001 [DIRS 185573]).

2. Type of Data Qualification Method(s) [Including rationale for selection of method(s) (Attachment 3) and qualification attributes (Attachment 4)]

Method: Corroborating data (Method 4), Technical Assessment (Method 5)
Rationale:
a. Corroborating data are available for comparison with subsets of the unqualified data - Ba on zeolitic tuff in J-13 water (DTN: LA0407AM831341.001 [DIRS 170623]) and U on devitrified tuff in J-13 water [DTN: LA0407AM831341.006 [DIRS 170628].
b. Inferences drawn to corroborate the unqualified data can be clearly identified, justified, and documented.

Qualification Process Attributes:
5. Quality and reliability of the measurement control program under which the data were generated
10. Extent and quality of corroborating data

3. Data Qualification Team and Additional Support Staff Required
Sharad Kelkar, Arend Meijer

4. Data Evaluation Criteria

1. Data to be compared shall have the same range as the corroborating data. The differences between the unqualified and the corroborating data are less than the inherent uncertainty which is one order of magnitude.
2. The technical adequacy of equipment and procedures used to collect and analyze the data.

5. Identification of Procedures Used
SCI-PRO-001 REV007

6. Plan coordinated with the following known organizations providing input to or using the results of the data qualification
N/A

Section III. Approval

Qualification Chairperson Printed Name	Qualification Chairperson Signature	Date
Sharad Kelkar	Sharad Kelkar	08/27/2008
Responsible Manager Printed Name	**Responsible Manager Signature**	**Date**
Robert MacKinnon	Robert MacKinnon	10/02/08

SCI-PRO-001.1-R1

ATTACHMENT A – CORRECTIONS TO SECTION 6.4.2 OF MDL-NBS-HS-000010 REV 03 AD 01 TO ADDRESS CR 12360

6.4.2.2 Form of the Dispersion Tensor for Axisymmetric Media

Generally, the porewater velocity and the dispersion tensor vary spatially and temporally. Experimental studies of transport in groundwater have determined the nature of the dispersion tensor and the appropriate values of the dispersivity parameter. Gelhar (1997 [DIRS 145122], p. 164, Figure 8) showed that distinct values of the longitudinal dispersivity, the transverse dispersivity in the horizontal direction, and the transverse dispersivity in the vertical direction can be identified based on available field transport studies. The general conceptual model underlying the use of these three terms is one of horizontal flow with tortuous fine-scale flow through heterogeneous media. The details of transport through the heterogeneous media give rise to the spreading of solute in the direction of flow and, to a lesser extent, transverse to the direction of flow. Of course, groundwater flow, though generally horizontal, exhibits vertical velocities locally in regions of upward or downward gradients, such as in areas of recharge or discharge or when the flow is subject to variability in hydraulic conductivity that diverts water vertically.

Tompson et al. (1987 [DIRS 145195], Appendix A and Equation A1) discuss the application of a dispersion tensor for randomly heterogeneous porous media. They present a dispersion tensor that incorporates a longitudinal dispersivity and a transverse dispersivity that is independent of the flow orientation:

$$\overline{D} = \alpha_T v \overline{I} + (\alpha_L - \alpha_T) \overline{vv} / v \qquad \text{(Eq. 2)}$$

Where $\overline{D}$ is the dispersion tensor, $\overline{I}$ is the identity tensor, α_L is the longitudinal dispersivity, and α_T is the transverse dispersivity.

Burnett and Frind (1987 [DIRS 130526], Equations 6a to 6f) proposed a generalization of this tensor for axisymmetric media, to account for different values of transverse dispersivities in the horizontal and vertical directions as observed in natural stratified media with flow along the bedding plane (for example, Zheng and Bennett 1995 [DIRS 154702], pp. 45 to 46). In practice, while available data to determine the alternate dispersivity values from field observations are limited, it is possible that more complex forms better represent the complexity and variety of different heterogeneities present in natural systems. An important conclusion from the available field data is that longitudinal dispersion is a strong function of scale, that is, the travel length of a solute plume in the medium (e.g., Neuman 1990 [DIRS 101464], Figure 1). In a typical groundwater flow model at the scale of a flow basin, characteristic flow distances of tens to hundreds of meters vertically may be present, compared to hundreds to thousands of meters horizontally. Given the difference in scale, it is not clear that the longitudinal dispersivity in the vertical direction should be set equal to that in the horizontal direction. In addition, in stratified porous media containing heterogeneities such as irregularly shaped beds or clay lenses, the characteristic scale of the heterogeneity encountered by a solute will be different in the horizontal and vertical directions, yielding potentially different values for longitudinal

dispersion. This was the motivation for deriving a general form of the dispersion tensor for an axisymmetric medium (a medium that displays rotational symmetry about an axis) as presented by Lichtner et al. (2002 [DIRS 163821], Equations 1 and 47). This form of the dispersion tensor allows the longitudinal dispersivity in the vertical direction to be different from that in the horizontal direction. While quite general, this formulation requires the specification of four independent parameters, limiting the use of this approach in practical problems. In situations where the axis of symmetry is vertical and the flow fields are horizontal to subhorizontal, as is the case at Yucca Mountain presented in *Saturated Zone Site-Scale Flow Model* (SNL 2007 [DIRS 177391], Section 6.5), the generalized tensor agrees with that given by Burnett and Frind (1987 [DIRS 130526], Equations 6a to 6f).

In applications to random walk particle tracking, the dispersion tensor is not used directly, but a displacement matrix must be derived for use with the Langevin equation. This development is presented in the next section.

6.4.2.3 Random-Walk Particle-Tracking Method

Given a steady-state velocity field generated, for example, for an arbitrary permeability field, a random walk is superimposed on the flow field to describe dispersion and molecular diffusion. The general approach used in particle tracking is to replace the partial differential equation for the solute concentration, C, generally expressed by Equation 1, with random-walk displacements defined in differential form by the Langevin equation for position vector $x(t)$ (Gardiner 1997 [DIRS 145116], p. 80):

$$dx = A(x,t)dt + B(x,t)dW(t) \tag{Eq. 3}$$

The matrix A represents the deterministic background displacement determined by $\bar{v}$ and, in addition, contains contributions from the dispersion tensor. The displacement matrix B refers to a stochastic random-walk process that incorporates molecular diffusion and dispersion. The differential $dW(t)$ represents a Wiener process describing Brownian motion with the properties:

$$< dW >= 0 \tag{Eq. 4}$$

and

$$< dW(t)dW(t) >= Idt \tag{Eq. 5}$$

where the angular brackets represent the ensemble mean.

The equivalent Fokker-Planck equation corresponding to the Langevin equation for the conditional probability $P(x,t|x_0,t_0)$ is given by (Gardiner 1997 [DIRS 145116], p. 97):

$$\frac{\partial P}{\partial t} = -\nabla \cdot \left[A(x,t)P\right] + \nabla : \nabla \left[\frac{1}{2} B\widetilde{B}P\right] \tag{Eq. 6}$$

where $\tilde{B}$ represents the transpose of the B matrix. The Fokker-Planck equation may be written in the form of the transport equation by rearranging Equation 6 to obtain:

$$\frac{\partial P}{\partial t} = -\nabla \cdot \left[\left(A(x,t) - \frac{1}{2} \nabla \cdot B\tilde{B} \right) P \right] + \nabla \cdot \left[\frac{1}{2} B\tilde{B} \nabla P \right] \quad \text{(Eq. 7)}$$

Comparing this modified Fokker-Planck equation with the continuum-based transport equation given in Equation 1 yields the identifications:

$$P(x,t \mid x_0,t_0) = \frac{N_A}{N} C(x,t), \quad \text{(Eq. 8)}$$

where N represents the number of particles and N_A denotes Avogadro's number,

$$A(x,t) = \vec{v} + \nabla \cdot D \quad \text{(Eq. 9)}$$

and

$$\frac{1}{2} B\tilde{B} = D \quad \text{(Eq. 10)}$$

Therefore, it is necessary to obtain the displacement matrix B based on the dispersion tensor D. To do this, the approach used by Tompson et al. (1987 [DIRS 145195], Appendix A) is followed in which a transformation that diagonalizes the dispersion tensor is carried out. By construction, the eigenvectors of the dispersion tensor depend only on the components of the flow velocity but not on the dispersivity values themselves. One eigenvector always points in the direction of the flow velocity. The other two eigenvectors are perpendicular to the direction of flow. The eigenvalue problem for D reads:

$$De_\lambda = \lambda \bar{e}_\lambda \quad \text{(Eq. 11)}$$

with eigenvalue λ and eigenvector $\bar{e}_\lambda$. Because the dispersion tensor is symmetric (Bear 1972 [DIRS 156269], p. 611), there exists an orthogonal transformation U that diagonalizes D (Tompson et al. 1987 [DIRS 145195], p. 106, Equation A-3):

$$\tilde{U}DU\tilde{U}e_\lambda = \lambda \tilde{U}\bar{e}_\lambda \quad \text{(Eq. 12)}$$

where $\tilde{U}$ is the transpose of U, with:

$$\tilde{U}DU = \hat{D} \quad \text{(Eq. 13)}$$

where $\hat{D}$ is a diagonal matrix, and U satisfies the relations:

$$U\tilde{U} = \tilde{U}U = I \quad \text{(Eq. 14)}$$

Expressing $\hat{D}$ in the form:

$$\hat{D} = Q\tilde{Q} \quad \text{(Eq. 15)}$$

with Q diagonal, then gives:

$$2D = 2U\hat{D}\tilde{U} = 2UQ\tilde{Q}\tilde{U} = B\tilde{B} \quad \text{(Eq. 16)}$$

From this relation it follows that the displacement matrix B is given by (Tompson et al. 1987 [DIRS 145195], p. 107, Equation A10):

$$B = \sqrt{2}UQ \quad \text{(Eq. 17)}$$

The implementation of the particle-tracking model requires a finite difference form of Equation 3 at time step *n*, which in this model is given by:

$$X_i^n = X_i^{n-1} + A_i\Delta t + \sqrt{\Delta t}\sum_j B_{ij}Z_j \quad \text{(Eq. 18)}$$

with

$$dW_j = Z_j\sqrt{\Delta t} \quad \text{(Eq. 19)}$$

for a time step Δt, where Z_j represents a uniform random number occurring with unit probability over the interval $-\frac{1}{2}$ to $\frac{1}{2}$.

The final step in the derivation is to determine the form of the displacement matrix B. Since the SZ Transport model needs to accommodate different values of the transverse dispersivity in the vertical and horizontal directions, Equations A13a, A13b and an approximate generalization of the Equation A11 of Tompson et al. (1987 [DIRS 145195]) were used, leading to Equation 20 below:

$$B = \begin{pmatrix} \frac{\nu_1}{\nu}\sqrt{2(\alpha_L\nu + D_0)} & -\frac{\nu_2\sqrt{2(\alpha^H{}_T(\nu_1^2+\nu_2^2)+\alpha^v{}_T\nu 3^2 + D_0)}}{\sqrt{\nu^2+2\nu_1\nu_3+\nu_2^2}} & -\frac{(\nu_2^2+\nu_3^2+\nu_1\nu_3)\sqrt{2(\alpha^v{}_T\nu + D_0)}}{\nu\sqrt{\nu^2+2\nu_1\nu_3+\nu_2^2}} \\ \frac{\nu_2}{\nu}\sqrt{2(\alpha_L\nu + D_0)} & \frac{(\nu_1+\nu_3)\sqrt{2(\alpha^H{}_T(\nu_1^2+\nu_2^2)+\alpha^v{}_T\nu 3^2 + D_0)}}{\sqrt{\nu^2+2\nu_1\nu_3+\nu_2^2}} & \frac{\nu_2(\nu_1+\nu_3)\sqrt{2(\alpha^v{}_T\nu + D_0)}}{\nu\sqrt{\nu^2+2\nu_1\nu_3+\nu_2^2}} \\ \frac{\nu_3}{\nu}\sqrt{2(\alpha_L\nu + D_0)} & -\frac{\nu_2\sqrt{2(\alpha^H{}_T(\nu_1^2+\nu_2^2)+\alpha^v{}_T\nu 3^2 + D_0)}}{\sqrt{\nu^2+2\nu_1\nu_3+\nu_2^2}} & \frac{(\nu_1^2+\nu_2^2+\nu_1\nu_3)\sqrt{2(\alpha^v{}_T\nu + D_0)}}{\nu\sqrt{\nu^2+2\nu_1\nu_3+\nu_2^2}} \end{pmatrix} \quad \text{(Eq. 20)}$$

where D_0 is the molecular diffusivity. In summary, the particle trajectory is computed by a finite difference technique expressed in Equation 18. The first displacement term of Equation 18

($A\Delta t$) is deterministic, with A defined in Equation 9. This expression captures the movement of particles in the streamlines defined by the flow field. The term $\nabla \cdot D\Delta t$ is required to reproduce the transport equation correctly for cases in which there are gradients in velocity or dispersion coefficient. It reduces to zero for uniform flow fields and constant dispersivity. What is retained in this case is transport along the flow streamline governed by the flow field. The last term in Equation 18 is a stochastic random-walk term to simulate dispersion, with the form of the matrix B in Equation 20.

Determination of the advection portion of the deterministic term $A\Delta t$ requires that the velocity at the particle location be determined. In this version of the code FEHM, the method is restricted to orthogonal finite-element grids. This simplification means that the control volume associated with each grid point is a brick-shaped element. Velocity interpolation within a cell is then determined quickly and easily using the velocity interpolation scheme first derived by Pollock (1988 [DIRS 101466], Equations 4a to 5c). Using that scheme, the code determines, for a given particle at a given location within the cell, the time required to exit the cell and the location where it leaves. If this time is greater than the time step Δt, the particle location within the cell is computed. If the time is less than the time step Δt, the particle is forced to stop at this location and then proceed in another step within the adjoining cell. This process is repeated until the ending time Δt is reached. At the end of this time step, the term $\nabla \cdot D\Delta t$ is used to move the particle deterministically to correct for gradients in the dispersion coefficient. A differencing scheme on the finite-element grid using a trilinear interpolation analogous to the method described by LaBolle et al. (1996 [DIRS 105039], pp. 587 to 588) is used to compute these terms, with the modification that the interpolated quantity is the local Darcy flux rather than the fluid velocity. This modification yields smoother results in situations such as those encountered at volcanic rock-alluvium interfaces, where local porosity can change by several orders of magnitude from a node to its neighbor. Finally, the random-walk term is applied (the final term in Equation 18) using the B matrix derived above (Equation 20).

For this method to work properly, the time step must be selected such that, on average, a particle takes several time steps within each cell. In a system with large variations in porewater velocity due to permeability and porosity differences from cell to cell, the appropriate time step can vary greatly throughout the domain. In FEHM, this factor is accounted for by dynamically determining the characteristic time step in an approach similar to that developed by Wen and Gomez-Hernandez (1996 [DIRS 130510], p. 137). In a given cell, the magnitude of the velocity in the cell is used to scale the time step. The time required to traverse the cell completely in each of the three coordinate directions is computed, and the minimum is determined. Then a user-defined parameter called the Courant factor is multiplied by this minimum time to obtain the time step for the particle within the cell. This approach ensures that several steps are taken by a particle within a cell but minimizes computational time by tailoring each time step to the characteristic velocities within the cells.

Applying the random-walk method on grids and flow fields, it was found that the theoretically simple inclusion of the $\nabla \cdot D$ term to correct for velocity gradients may not be sufficient to account for regions with highly variable velocity fields. In short, computation of $\nabla \cdot D$ on the scale of the finite-element grid may not be sufficient to capture the magnitude of this term adequately. For example, in high-permeability zones immediately adjacent to confining units of low permeability, the gradient is not captured sufficiently accurately to prevent the artificial

meandering of a small number of particles into the low-permeability region. As a result, some particles are held up for an unrealistically long time in these zones, resulting in a nonconservative tailing of the solute BTC at a downstream location. To correct this problem, a user-defined velocity-scaling parameter can be defined to prohibit particles from entering the low-velocity domain by random-walk processes. If the ratio of the velocity before and after the random-walk jump is less than this parameter, the code prohibits the jump, and the particle is returned to the original position where another jump is taken with a different set of random numbers.

The particle tracking method presented here, as discussed by Lichtner et al. (2002 [DIRS 163821]), has the advantage that solute mass is automatically conserved as long as the number of particles is tracked in the numerical implementation, and the method is free from numerical convergence and numerical dispersion problems encountered by the methods that use the approach of solving discretized forms of the advection dispersion equation (Equation 1). Further, the boundary conditions described in Section 6.3 are easily implemented by removing from further computations any particles that reach a model boundary.

To report the results of a particle-tracking simulation, two options are available. The first requires the definition of a zone consisting of a set of finite-element grid points representing a portion of the model domain where transport results are desired. For example, a "boundary of the accessible environment" compliance boundary, which is a given distance from the repository, can be defined by listing all of the nodes in the boundary. Then the code determines the first arrival time of each particle at any node in this fence and reports the cumulative arrival time distribution for all particles. This arrival-time distribution can then be converted to a groundwater concentration using a representative volume of 3,000 acre-feet in accordance with 10 CFR 63.312 [DIRS 180319], and the resulting curve can be used as the input to the performance assessment analysis. Alternatively, the concentration of particles at any cell in the finite-element domain can be reported as the number of particles residing in the cell divided by the fluid mass in the cell. Concentrations computed in this way represent the in situ concentration in response to the injection of a pulse of solute at time zero. To obtain the cumulative BTC, a time integration of these results may be performed, yielding the in situ concentration BTC at the node in response to a step change in concentration.